

A Survey on Generative Diffusion Model

Hanqun Cao, Cheng Tan, Zhangyang Gao, Guangyong Chen, Pheng-Ann Heng, *Senior Member, IEEE*, and Stan Z. Li, *Fellow, IEEE*

Abstract—Deep learning shows excellent potential in generation tasks thanks to deep latent representation. Generative models are classes of models that can generate observations randomly with respect to certain implied parameters. Recently, the diffusion Model has become a rising class of generative models by virtue of its power-generating ability. Nowadays, great achievements have been reached. More applications except for computer vision, speech generation, bioinformatics, and natural language processing are to be explored in this field. However, the diffusion model has its genuine drawback of a slow generation process, single data types, low likelihood, and the inability for dimension reduction. They are leading to many enhanced works. This survey makes a summary of the field of the diffusion model. We first state the main problem with two landmark works – DDPM and DSM, and a unified landmark work – Score SDE. Then, we present classified improved techniques for existing problems in the diffusion-based model field. For model speed-up improvement, we present a diverse range of advanced techniques to speed up the diffusion models – training schedule, training-free sampling, mixed-modeling, and score & diffusion unification. For data structure diversification, we present improved techniques for applying diffusion models in continuous space, discrete space, and constraint space. For likelihood optimization, we present theoretical methods for improving ELBO and minimizing the variational gap. For dimension reduction, we present several techniques to solve the high dimension problem. Regarding existing models, we also provide a benchmark of FID score, IS, and NLL according to specific NFE. Moreover, applications with diffusion models are introduced including computer vision, sequence modeling, audio, and AI for science. Finally, there is a summarization of this field together with limitations & further directions. Summation of existing well-classified methods is in our Github: <https://github.com/chq1155/A-Survey-on-Generative-Diffusion-Model>.

Index Terms—Diffusion Model, advanced improvement on diffusion, diffusion application.

1 INTRODUCTION

How can we empower machines with human-like imagination? Deep generative models, e.g., VAE [1], [2], [3], [4], EBM [5], [6], [7], [8], GAN [9], [10], [11], [12], [13], normalizing flow [14], [15], [16], [17], [18], [19] and diffusion models [20], [21], [22], [23], [24], have shown great potential in creating new patterns that humans cannot properly distinguish. We focus on diffusion-based generative models, which do not require aligning posterior distributions as VAE, dealing with intractable partition functions as EBM, training additional discriminators as GAN, or imposing network constraints as normalizing flow. Thanks to the aforementioned virtues, diffusion-based methods have drawn considerable attention from computer vision, and natural language processing to graph analysis. However, there is still a lack of systematic taxonomy and analysis of research progress on diffusion models.

Advances in the diffusion model have provided tractable probabilistic parameterization for describing the model, a

stable training procedure with sufficient theoretical support, and a unified loss function design with high simplicity. The diffusion model aims to transform the prior data distribution into random noise before revising the transformations step by step to rebuild a brand new sample with the same distribution as the prior [25]. In recent years, the diffusion model has displayed its exquisite potential in the field of computer vision (CV) [20], [26], [27], [28], [29], [30], [31], [32], [33], [34], [35], [36], [37], [38], sequence modeling [39], [40], [41], [42], audio processing [43], [44], [45], [46], [47], [48], [49], [50], [51], [52], and AI for science [53], [54], [55], [56], [57]. Inspired by the so-far successes of the diffusion model in these popular domains, applying diffusion models to generation-related tasks of the other domains would be a favorable path for exploiting powerful generative capacity.

On the other hand, the diffusion model has the inherent drawback of plenty of sampling steps and a long sampling time compared to Generative Adversarial Networks (GANs) and Variational Auto-Encoders (VAEs). Since diffusion models leverage a Markov process to convert data distribution via tiny perturbations, a large number of diffusion steps are required in both the training and inference phases. Thus, it takes more time to sample from a random noise until it eventually alters to high-quality data similar to the prior. Furthermore, other problems such as likelihood optimization and the inability of dimension reduction also count. Therefore, lots of works aspired to accelerate the diffusion process along with improving sampling quality [61], [62], [63]. For example, DPM-solver takes advantage of ODE's stability to generate samples of the State-of-the-art within 10 steps [64]. D3PM [65] proposes not only hybrid training loss but also text & categorical data. We summarize im-

- H. Cao is with the Department of Math, The Chinese University of Hong Kong, Hong Kong, China, also with Zhejiang Lab, Hangzhou, China, and the AI Lab, School of Engineering, Westlake University, Hangzhou, China. Email: 1155141481@link.cuhk.edu.hk.
- C. Tan and Z. Gao are with Zhejiang University, Hangzhou, China, and also with the AI Lab, School of Engineering, Westlake University, Hangzhou, China. Email: tancheng, gaozhangyang@westlake.edu.cn.
- G. Chen is with Zhejiang Lab, Hangzhou, China. Email: gy-chen@zhejianglab.com.
- P.-A. Heng is with the Department of Computer Science and Engineering, The Chinese University of Hong Kong, Hong Kong, China.
- Stan Z. Li is with the AI Lab, School of Engineering, Westlake University, Hangzhou, China. Email: Stan.ZQ.Li@westlake.edu.cn.
- H. Cao, C. Tan, and Z. Gao contributed equally to this work.

Manuscript received April 19, 2005; revised August 26, 2015.

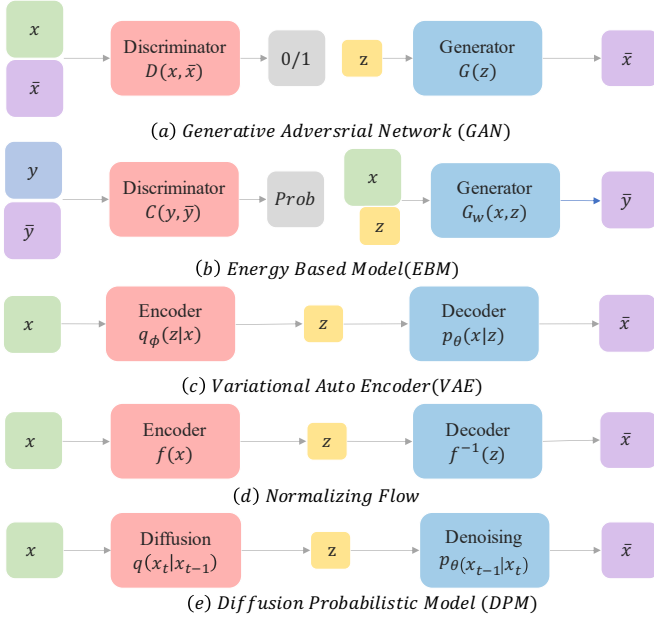


Fig. 1. Generative Models Pipeline. **(a)** Generative Adversarial Net (GAN) [58] applies adversarial training strategy onto the generator to generate lifelike samples like input distributions. **(b)** Energy-Based Model (EBM) [59] designs a suitable energy function for pair-wise energy matching between conditions and samples, similar to a generative discriminator in GAN. **(c)** Variational Auto-Encoder (VAE) [60] applies the encoder to project the prior into a latent space with reduced dimension from which the decoder can sample. **(d)** Normalizing flow (NF) [18] employs a well-designed reversible flow function for turning input into latent variable before returning to samples with the inverse of flow function. **(e)** Diffusion model gradually injects noise into the original data until it turns to the known noise distribution before reversing each step in the sampling steps.

provement works on diffusion models into four classes. (1) Speed-up improvement, (2) Data structure diversification, (3) Likelihood optimization, and (4) Dimension reduction. The detailed contents are provided in Section 3.

Hence, based on the wide range of applications along with multi-perspective thinking on algorithm improvement, we target to provide a detailed survey about current aspects of diffusion models. By classifying enhanced algorithms and applications in other domains, the core contributions of this review are as follows:

- Summarize essence mathematical formulation and derivation of fundamental algorithms in the field of diffusion model, including taking advantage of training strategy, and sampling algorithm.
- Present comprehensive and up-to-date classification of improved diffusion algorithms and divide them into four proposes, which are speed-up improvement, structure diversification, likelihood optimization, and dimension reduction.
- Provide extensive statements about the application of diffusion models on computer vision, natural language processing, bioinformatics, and speech processing which include domain-specialized problem formulation, related datasets, evaluation metrics, and downstream tasks, along with sets of benchmarks.
- Clarify current limitations of models and possible further-proof directions concerning the field of diffusion models.

2 PROBLEM STATEMENT

2.1 Notions and Definitions

2.1.1 State

States are a set of data distributions that describe the whole process of diffusion models. The noise is gradually injected into the starting distribution, called starting state x_0 . With enough steps of noise injection, the distribution finally comes into a known noise distribution (mostly Gaussian), which is called the prior state x_T (Discrete)/ x_1 (Continuous). Then, the other distributions between the starting state and the prior state are called intermediate states x_t .

2.1.2 Process & Transition Kernel

Forward & Reverse Process & Kernel: The process that transforms the starting state into the tractable noise is the forward/diffusion process F . The process following the opposite direction to the forward process is called reverse/denoised process R . The reverse process samples the noise gradients step by step into the samples as the starting state. In either process, the interchange between any two states is achieved by the transition kernel. To present a unified framework, the forward process consists of plenty of forward steps which are the forward transition kernels. The reverse process conducts similarly:

$$F(x, \sigma) = F_T(x_{T-1}, \sigma_T) \cdots \circ F_t(x_{t-1}, \sigma_t) \cdots \circ F_1(x_0, \sigma_1) \quad (1)$$

$$R(x, \sigma) = R_1(x_1, \sigma_1) \cdots \circ R_t(x_t, \sigma_t) \cdots \circ R_T(x_T, \sigma_T) \quad (2)$$

$$x_t = F_t(x_{t-1}, \sigma_t), \quad x_{t-1} = R_t(x_t, \sigma_t) \quad (3)$$

Different from the discrete case, for any time $0 \leq t < s \leq 1$, the forward process is defined:

$$F(x, \sigma) = F_{s1}(x_s, \sigma_{s1}) \circ F_{ts}(x_t, \sigma_{ts}) \circ F_{0t}(x_0, \sigma_{0t}) \quad (4)$$

$$R(x, \sigma) = R_{t0}(x_t, \sigma_{t0}) \cdots \circ R_{st}(x_s, \sigma_{st}) \cdots \circ R_{1s}(x_T, \sigma_{1s}) \quad (5)$$

$$x_s = F_{ts}(x_s, \sigma_{ts}), \quad x_t = R_{st}(x_s, \sigma_{st}) \quad (6)$$

where F_t, R_t are the forward and reverse transition kernel at time t with the variables intermediate state x_{t-1} & x_t and the noise scale σ_t . The most frequently used kernel is the Markov kernel since it ensures randomness and tractability in the forward process and the reverse process. The difference between this expression and normalizing flow is the variable noise scale, which controls the randomness of the whole process. When the noise is close to 0, the process will become the normalizing flow which is deterministic.

Pipeline: Denote the sampled data as \tilde{x}_0 the generalized process can be expressed as:

$$\tilde{x}_0 = [R_1(x_1, \sigma_1) \cdots \circ R_t(x_t, \sigma_t) \cdots \circ R_T(x_T, \sigma_T)] \circ [F_T(x_{T-1}, \sigma_T) \cdots \circ F_t(x_{t-1}, \sigma_t) \cdots \circ F_1(x_0, \sigma_1)] \quad (7)$$

$$\tilde{x}_0 = [R_{t0}(x_t, \sigma_{t0}) \cdots \circ R_{st}(x_s, \sigma_{st}) \cdots \circ R_{1s}(x_T, \sigma_{1s})] \circ [F_{s1}(x_s, \sigma_{s1}) F_{0t} \circ F_{ts}(x_t, \sigma_{ts}) \circ F_{0t}(x_0, \sigma_{0t})] \quad (8)$$

2.1.3 Discrete and continuous

Taking the perturbation kernel to sufficiently small, the whole discrete process will contain infinite steps. To tackle the mechanism behind this situation, the continuous process starting from time 0 and ending at time 1 is sued in many improved algorithms [66], [67] to obtain better performance. Compared to a discrete process, the continuous one enables the extraction of any information from any time state. Further, assuming the change of perturbation kernel is slight enough, the continuous process enjoys better theoretical support.

2.1.4 Training Objective

The diffusion model as one type of the generative model follows the same training objective as variational autoregressive-encoder and normalizing flow, which is keeping starting distribution x_0 and sample distribution \tilde{x}_0 as close as possible. This is implemented by maximizing the log-likelihood [25]:

$$\mathbb{E}_{F(x_0, \sigma)} [-\log R(x_T, \tilde{\sigma})] \quad (9)$$

where the $\tilde{\sigma}$ in the reverse process differs from the one in the forward process.

2.2 Problem Formulation

2.2.1 Denoised Diffusion Probabilistic Model

DDPM Forward Process: Based on the unified framework, DDPM chooses a sequence of noise coefficients $\beta_1, \beta_2, \dots, \beta_T$ for Markov transition kernels following specific patterns. The common choices are constant schedule, linear schedule, and cosine schedule. According to [68], different noise schedules have no clear effects in experiments. The DDPM forward steps are defined as:

$$F_t(x_{t-1}, \beta_t) := q(x_t | x_{t-1}) := \mathcal{N}(x_t, \sqrt{1 - \beta_t}x_{t-1}, \sqrt{\beta_t}\mathbf{I}) \quad (10)$$

By a sequence of diffusion steps from x_0 to x_T , we have the Forward Diffusion Process:

$$F(x_0, \beta) := q(x_{1:T} | x_0) := \prod_{t=1}^T q(x_t | x_{t-1}) \quad (11)$$

DDPM Reverse Process: Given the Forward Process above, we define the Reverse Process with learnable Gaussian transitions parameterized by θ [68]:

$$R_t(x_t, \Sigma_\theta) := p_\theta(x_{t-1} | x_t) := \mathcal{N}(x_{t-1}; \mu_\theta(x_t, t), \Sigma_\theta(x_t, t)) \quad (12)$$

By a sequence of reverse steps from x_T to x_0 , we have the reverse process starting at $p(x_T) = \mathcal{N}(x_T; \mathbf{0}, \mathbf{I})$:

$$R(x_T, \Sigma_\theta) := p_\theta(x_{0:T}) := p(x_T) \prod_{t=1}^T p_\theta(x_{t-1} | x_t) \quad (13)$$

Consequently, the distribution $p_\theta(x_0) = \int p_\theta(x_{0:T}) dx_{1:T}$ should be the distribution of \tilde{x}_0 .

Notations	Descriptions
T	Discrete total time steps
t	Random time t
z_t	Random noise with normal distribution
ϵ	Random noise with normal distribution
\mathcal{N}	Normal distribution
β	Generalized process noise scale
β_t	Variance scale coefficients
$\beta(t)$	Continuous-time β_t
σ	Generalized process noise scale
σ_t	Noise scale of perturbation
$\sigma(t)$	Continuous-time σ_t
α_t	Mean coefficient defined as $1 - \beta_t$
$\alpha(t)$	Continuous-time α_t
$\tilde{\alpha}_t$	Cumulative product of α_t
$\gamma(t)$	Signal-to-Noise ratio
η_t	Step size of annealed Langevin dynamics
x	Unperturbed data distribution
\tilde{x}	Perturbed data distribution
x_0	Starting distribution of data
x_t	Diffused data at time t
x'_t	Partly diffused data at time t
x_T	Random noise after diffusion
$F(x, \sigma)$	Forward/Diffusion process
$R(x, \sigma)$	Reverse/Denoised process
$F_t(x_t, \sigma_t)$	Forward/Diffusion step at time t
$R_t(x_t, \sigma_t)$	Reverse/Denoised step at time t
$F_{ts}(x_t, \sigma_{ts})$	Forward/Diffusion step at time t
$R_{st}(x_s, \sigma_{st})$	Reverse/Denoised step at time t
$q(x_t x_{t-1})$	DDPM forward step at time t
$p(x_{t-1} x_t)$	DDPM reverse step at time t
$f(x, t)$	Drift coefficient of SDE
$g(t)$	Simplified diffusion coefficient of SDE
$\mathcal{D}(x, t)$	Degrader at time t in Cold Diffusion
$\mathcal{R}(x, t)$	Reconstructor at time t in Cold Diffusion
w, \tilde{w}	Standard Wiener process
$\nabla_x \log p_t(x)$	Score function w.r.t x
$\mu_\theta(x_t, t)$	Mean coefficient of reversed step
$\Sigma_\theta(x_t, t)$	Variance coefficient of reversed step
$\epsilon_\theta(x_t, t)$	Noise prediction model
$s_\theta(x)$	Score network model
L_0, L_{t-1}, L_T	Forward loss, reversed loss, decoder loss
L_{vlb}	Evidence Lower Bound
L_{vlb}^{CT}	Continuous evidence lower bound
L_{simple}	Simplified denoised diffusion loss
L_{simple}^{CT}	Continuous L_{simple}
L_{Gap}	Variational gap
L_{KID}	Kernel inception distance
$L_{Recovery}$	Recovery likelihood loss
L_{hybrid}	Hybrid diffusion loss
$L_{DDPM\&GAN}$	DPM ELBO and GAN hybrid loss
$L_{DDPM\&VAE}$	DPM ELBO and VAE hybrid loss
$L_{DDPM\&Flow}$	DPM ELBO and normalizing flow hybrid loss
L_{DSM}	Loss of denoised score matching
L_{ISM}	Loss of implicit score matching
L_{SSM}	Loss of sliced score matching
$L_{Distill}$	Diffusion distillation loss
$L_{DDPM\&Noise}$	DPM ELBO and reverse noise hybrid loss
L_{square}	Noise square loss
$L_{Trajectory}$	Process optimization loss
$L_{DDPM\&Class}$	DPM ELBO and classification hybrid loss
θ	learnable parameters
ϕ	learnable parameters

Diffusion Training Objective: By minimizing the negative log-likelihood (NLL), the minimization problem can be formulated as:

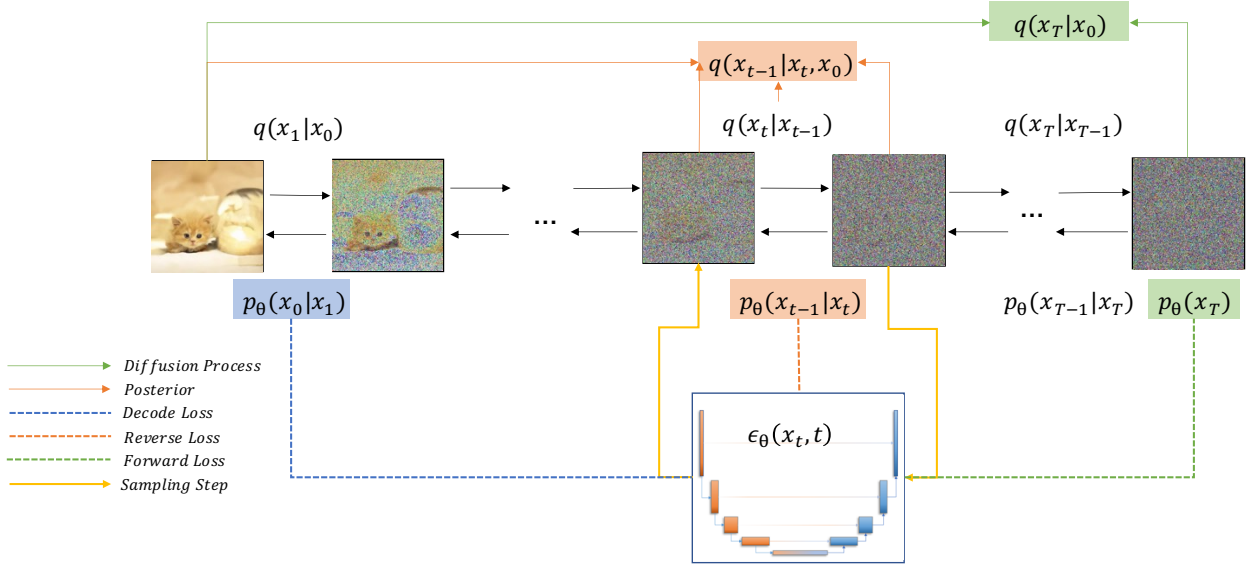


Fig. 2. Pipeline of Denoised Diffusion Probabilistic Model. The arrows pointing from left to right indicate the diffusion process and the arrows pointing in the reverse direction indicate the reverse process. The colored background transition terms are components of ELBO: the blue part stands for decode loss L_0 , the green part represents forward loss L_T , and the orange part constitutes the reverse loss L_t . Dashed lines with different colors show the training pattern of the noise prediction model ϵ_θ . Besides, in any step $1 \leq t \leq T$, the yellow lines denote the ancestral sampling process.

$$\begin{aligned}
 \mathbb{E}[-\log p_\theta(x_0)] &\leq \mathbb{E}_q \left[-\log \frac{p_\theta(x_{0:T})}{q(x_{1:T} | x_0)} \right] \\
 &= \mathbb{E}_q \left[-\log p(x_T) - \sum_{t \geq 1} \log \frac{p_\theta(x_{t-1} | x_t)}{q(x_t | x_{t-1})} \right] \\
 &= \mathbb{E}_q \left[\underbrace{D_{\text{KL}}(q(x_T | x_0) \| p(x_T))}_{L_T} \right. \\
 &\quad \left. + \sum_{t \geq 1} \underbrace{D_{\text{KL}}(q(x_{t-1} | x_t, x_0) \| p_\theta(x_{t-1} | x_t))}_{L_{t-1}} \right. \\
 &\quad \left. - \underbrace{\log p_\theta(x_0 | x_1)}_{L_0} \right] \\
 &=: L
 \end{aligned} \tag{14}$$

Here we use the symbol of Ho *et al.* [68]. Denote L_T as the prior loss. Denote L_0 as the reconstruction loss; Besides, denote $L_{1:T-1}$ as the consistent loss, which is the sum of the divergence between the posterior of the forwarding step and the corresponding reversing step.

2.2.2 Score Matching Formulation

The score matching model aims at solving the original data distribution estimation problem by approximating the gradient of data $\nabla_x \log p(x)$, which is called score. The main approach of score matching is to train a score network s_θ to predict the score [69], [70], which is obtained using perturbing data with different noise schedules. The score-matching process is defined as:

Score Perturbation Process & Kernel: The perturbation process consists of a sequence of perturbation steps with increasing noise scales $\sigma_1, \dots, \sigma_N$. The Gaussian perturbation kernel is defined as $q_{\sigma}(\tilde{x}|x) := \mathcal{N}(\tilde{x} | x, \sigma^2 I)$. For each noise scale σ_i , the score is equivalent to the gradient of the perturbation kernel. If we treat this increasing noise perturbation

as a discrete process, the transition kernel between two neighbor states is

$$x_i = x_{i-1} + \sqrt{\sigma_i^2 - \sigma_{i-1}^2} \epsilon, \quad i = 1, \dots, N \tag{15}$$

where N is the length of the noise scale sequence, and ϵ is random noise.

Score Matching Process: As noticed above, the goal of the score matching process is to obtain a score estimation network $s_\theta(x, \sigma)$ to be as close as possible to the gradient of perturbation kernel, which is

$$L := \frac{1}{2} \mathbb{E} \left[\|s_\theta(x, \sigma) - \nabla \log q(x)\|^2 \right] \tag{16}$$

where θ is the learnable parameters in the score network.

DDPM & DSM Connection: To some extent, score matching, and denoising diffusion are the same processes. **(1)** Denoising mechanism: both DSM and DDPM follow the pattern of fetching information during the noising process and reusing gradient during the denoising process. Moreover, noising schedule of DSM can be seen as an accumulation of constant-variance diffusion steps. **(2)** Training object: Both DSM and DDPM belong to a noise regression problem based on MLE. **(3)** Sampling method: both DSM and DDPM apply the idea of ancestral sampling, employing gradient to reconstruct the samples.

2.2.3 Score SDE Formulation

Score SDE [66] proposed a unified continuous framework based on the stochastic differential equation to describe diffusion and denoised score matching models. It not only presents the corresponding continuous set-up of DDPM of DSM based on score SDE but also proposes a density estimation ODE framework named probability flow ODE.

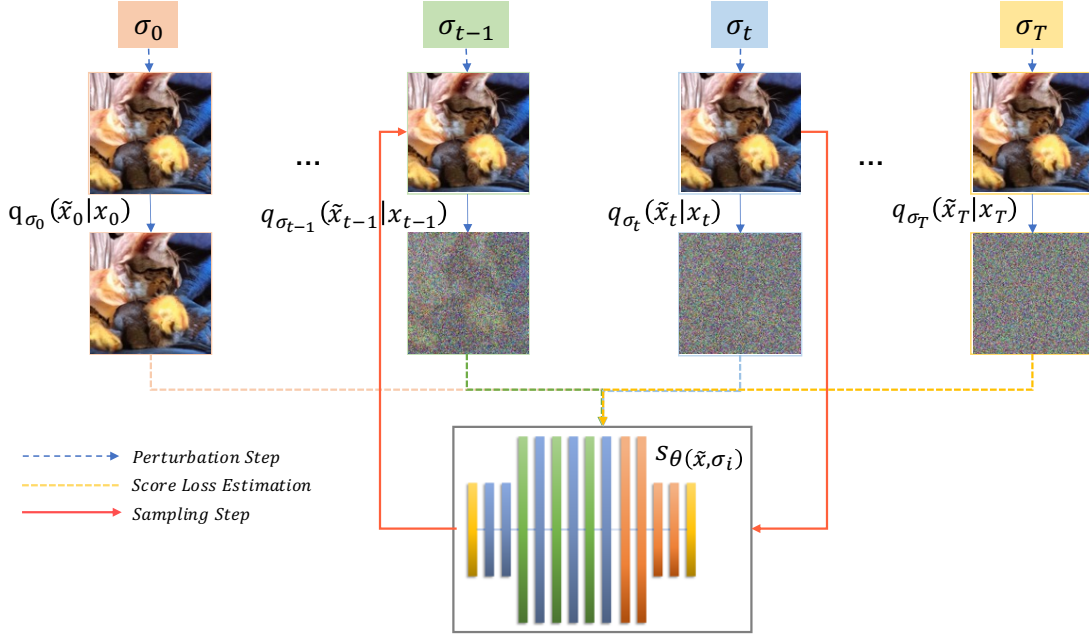


Fig. 3. Pipeline of Denoised Score Matching (DSM). The σ 's in different time states on the top represent alternative noise scales. The transition states $p_{\sigma_i}(\tilde{x}_i | x_i)$ are the output gradients of the perturbation. Dashed lines with different colors reveal that the scoring network s_θ is trained by minimizing the sum of L2-loss between the output gradient and the score in each noise scale. Besides, in any noise state $1 \leq t \leq T$, the red lines denote the Langevin Dynamics sampling process.

Forward Score SDE Process: In Song *et al.* [66], Diffusion process can be viewed as a continuous case described by Stochastic Differential Equation. And it is equal to the solution to Itô SDE [71], which is composed of a drift part for mean transformation and a diffusion coefficient for noise description. :

$$dx = f(x, t)dt + g(t)dw, t \in [0, T] \quad (17)$$

where w is the standard Wiener process/Brownian Motion, $f(\cdot, t)$ is the drift coefficient of $x(t)$, and $g(\cdot)$ is the simplified version of diffusion coefficient of $x(t)$, which is assumed not dependent on x . Besides, $p_0, p_t(x)$ denote the data distribution and probability density of $x(t)$. p_T denotes the original prior distribution which gains no information from p_0 . When the coefficients are piece-wise continuous, the forward SDE equation admits a unique solution [72].

Similar to the discrete case, the forward transition in the SDE framework is derived as:

$$\begin{aligned} F_{st}(x(s), g_{st}) &:= q(x_t | x_s) := \mathcal{N}(x_t | f_{ts}x_s, g_{ts}^2 I) \\ R_{ts}(x(t), g_{ts}) &:= q(x_s | x_t, x_0) \\ &= \mathcal{N}\left(x_s \mid \frac{1}{g_{t0}^2} \left(f_{s0}g_{ts}^2 x_0 + f_{ts}g_{s0}^2 x_t \right), \frac{g_{s0}^2 g_{ts}^2}{g_{t0}^2} I\right) \end{aligned} \quad (18)$$

$$\text{where } f_{ts} = \frac{f(x, t)}{f(x, s)} \text{ and } g_{ts} = \sqrt{g(t)^2 - f_{ts}^2 g(s)^2}.$$

Reversed Score SDE Process: In contrast to the Forward SDE Process, the Reversed SDE Process is defined with respect to the reverse-time Stochastic Differential Equation by running backward in time [66]:

$$dx = [f(x, t) - g(t)^2 \nabla_x \log p_t(x)] dt + g(t)d\bar{w}, t \in [0, T] \quad (19)$$

Furthermore, $\nabla_x \log p_t(x)$ is the score to be matched [73].

Score SDE Training Objective: The training objective of score SDE employs weighting scheme in the score loss compared to denoised score matching, which is

$$L := \mathbb{E}_t \{ \lambda(t) \mathbb{E}_{x(0)} \mathbb{E}_{x(t)|x(0)} \left[\|s_\theta(x(t), t) - \nabla_{x(t)} \log p(x(t)|x(0))\|_2^2 \right] \} \quad (20)$$

where $x(t), x(0)$ are corresponding continuous time variables of x_t, x_0 .

SDE-based DDPM & DSM: Based on the SDE frameworks, the transition kernel of DDPM and DSM can be expressed as :

$$dx = -\frac{1}{2}\beta(t)x dt + \sqrt{\beta(t)}dw \quad (21)$$

$$dx = \sqrt{\frac{d[\sigma^2(t)]}{dt}} dw \quad (22)$$

where $\beta(t)$ and $\sigma(t)$ are the continuous-time variable of discrete noise scales β_t and σ_i . Moreover, the two kinds of SDE are called Variation Preserving (VP) and Variation Explosion (VE) SDE respectively.

Probability Flow ODE: Probability Flow ODE (Diffusion ODE) [66] is the continuous-time ODE that supports the deterministic process which shares the same marginal probability density with SDE. Inspired by Maoutsa *et al.* [74] and Chen *et al.* [75], any type of diffusion process can be derived into a special form of ODE. In the case that functions G is independent of x , the probability flow ODE is

$$dx = \{f(x, t) - \frac{1}{2}G(t)G(t)^T \nabla_x \log p_t(x)\} dt \quad (23)$$

In contrast to SDE, probability flow ODE can be solved with larger step sizes as they have no randomness. Due to the advantages of ODE, several works such as PNDMs [76] and DPM-Solver [64] obtain amazing results by modeling the diffusion problem as an ODE.

2.3 Training Strategy

2.3.1 Denoising Diffusion Training Strategy

In order to minimize the negative log-likelihood, the only item we can be used to train is $L_{1:T-1}$. By parameterizing the posterior $q(x_{t-1}|x_t, x_0)$ using Baye’s rule, we have:

$$q(x_{t-1} | x_t, x_0) = \mathcal{N}(x_{t-1}; \tilde{\mu}_t(x_t, x_0), \tilde{\beta}_t I) \quad (24)$$

where α_t is defined as $1 - \beta_t$, $\bar{\alpha}_t$ is defined as $\prod_{k=1}^t \alpha_k$. Mean and variance schedules can be expressed as:

$$\begin{aligned} \tilde{\mu}_t(x_t, x_0) &:= \frac{\sqrt{\alpha_{t-1}}\beta_t}{1 - \bar{\alpha}_t}x_0 + \frac{\sqrt{\alpha_t}(1 - \bar{\alpha}_{t-1})}{1 - \bar{\alpha}_t}x_t \\ \tilde{\beta}_t &:= \frac{1 - \bar{\alpha}_{t-1}}{1 - \bar{\alpha}_t}\beta_t \end{aligned} \quad (25)$$

Keeping above parameterization as well as reparameterizing x_t as $x_t(x_0, \sigma)$, L_{t-1} can be regarded as an expectation of L2-loss between two mean coefficients:

$$L_{t-1} = \mathbb{E}_q \left[\frac{1}{2\sigma_t^2} \|\tilde{\mu}_t(x_t, x_0) - \mu_\theta(x_t, t)\|^2 \right] + C \quad (26)$$

Simplifying L_{t-1} by reparameterizing μ_θ w.r.t ϵ_θ , we obtain the simplified training objective named L_{simple} :

$$L_{simple} := \mathbb{E}_{x_0, \epsilon} \left[\frac{\beta_t^2}{2\sigma_t^2 \alpha_t (1 - \bar{\alpha}_t)} \right] \left\| \epsilon - \epsilon_\theta(\sqrt{\bar{\alpha}_t}x_0 + \sqrt{1 - \bar{\alpha}_t}\epsilon) \right\|^2 \quad (27)$$

Most diffusion models until now use the training strategy of DDPMs. But there exist some exceptions. DDIM’s training objective [77] can be transformed by adding a constant from DDPM’s although it is independent of Markovian step assumption; Training pattern of Improved DDPM [61] named as L_{hybrid} is to combine training object of DDPM L_{simple} and a term with variational lower bound L_{vlb} . However, L_{simple} still takes the main effect of these training methods.

2.3.2 Score Matching Training Strategy

Traditional score-matching techniques require massive computation cost for Hessian of log density function. To fix this problem, advanced methods find approaches to avoid Hessian computing. Implicit score matching (ISM) [73] treat the real score density as a non-normalized density function that can be optimized by neural network. Sliced score matching (SSM) [78] provide a unperturbed score estimation method through reverse-mode auto-differentiation by projecting score onto random vectors.

$$L_{ISM} := \mathbb{E} \left[\frac{1}{2} \|s_\theta(x)\|_\Lambda^2 + \nabla(s_\theta) \right] \quad (28)$$

$$L_{SSM} := \mathbb{E}_{p_v} \mathbb{E}_{p_{data}} \left[v^\top \nabla_x s_\theta(x) v + \frac{1}{2} \|s_\theta(x)\|_2^2 \right] \quad (29)$$

However, because of the low-manifold problem in real data as well as the sampling problem in the low-density region, denoised score matching could be the better solution for improving score matching. Denoised score matching (DSM) [69] transforms the original score matching into a perturbation kernel learning by perturbing a sequence of increasing noise.

$$L_{DSM} := \frac{1}{2} \mathbb{E}_{q_\sigma((\tilde{x}|x)p_{data}(x))} \left[\|s_\theta(\tilde{x}) - \nabla_{\tilde{x}} \log q_\sigma(\tilde{x}|x)\|_2^2 \right] \quad (30)$$

According to Song *et al.*, the noise distribution is defined to be $q_\sigma(\tilde{x}|x) = \mathcal{N}(\tilde{x}|x, \sigma^2 I)$. Thus, for each given σ , the specific expression denoising score matching objective is

$$L(\theta; \sigma) := \frac{1}{2} \mathbb{E}_{p_{data}(x)} \mathbb{E}_{\tilde{x} \sim \mathcal{N}(x, \sigma^2 I)} \left[\left\| s_\theta(\tilde{x}, \sigma) + \frac{\tilde{x} - x}{\sigma^2} \right\|_2^2 \right] \quad (31)$$

2.4 Sampling Algorithm

In the reverse process, the samples are rebuilt from random noise by extracting the gradient in each time step, which is called unconditional sampling. Besides, there is another class of sampling utilizing specific conditions. We call it conditional sampling. In this subsection, we present basic unconditional sampling algorithms for the three landmark works and effective conditional sampling algorithms in Appendix.

2.4.1 Unconditional Sampling

Ancestral Sampling The initial idea of ancestral sampling [79] is reconstructed with the gradient of inverse Markovian step by step.

Langevin Dynamics Sampling With a fixed step size $\epsilon > 0$, Langevin dynamics can produce samples from a probability density $p(x)$ through only the score function (Song *et al.*) $\nabla_x \log p(x)$.

Predictor-corrector (PC) Sampling PC sampling [80] is inspired by a type of ODE black-box ODE solver [81], [82], [83] to produce high-quality samples and trade-off accuracy for efficiency for all reversed SDE. The sampling procedure comprises a predictor sampler and a corrector sampler.

2.4.2 Conditional Sampling

Labeled Condition Sampling with labeled conditions provides gradient guidance in each sampling step. Usually, an additional classifier with UNet Encoder architecture for generating condition gradients for specific labels is needed. The labels can be text & categorical label [84], [85], [86], [87], [88], binary label [89], [90], or extracted features [26], [91], [92]. It is firstly presented by [84], and current conditional sampling methods are similar in theory.

Unlabeled Condition Except for label-guidance sampling, unlabeled condition sampling only takes self-information as guidance. Conducting in a self-supervised manner [93], [94], it is often applied in denoising [95], resolution [96], and inpainting [41] tasks.

3 ALGORITHM IMPROVEMENT

Nowadays, the main constraint of the diffusion model is its low speed and high computation cost. Although conditional diffusion with strong guidance can achieve high-fidelity samples within 10 steps [62], [97], unconditional sampling speed remains incomparable to GAN and VAE. Besides, handling diverse data distribution, optimizing log-likelihood, and dimension reduction techniques still count. In this section, we classify the improved algorithm w.r.t. the mainstream problems. For each problem, we present the significance and detailed taxonomy of improved techniques.

3.1 Speed-up Improvement

Although diffusion models enjoy high-fidelity generation, low sampling speed limits models' practicality. To improve this situation, advanced techniques can be divided into four categories, including training scheme enhancement, training-free accelerated sampling, mix-modeling design, and score-diffusion unification design.

3.1.1 Training Schedule

Improving the training schedule means modifying traditional training settings, such as diffusion schemes and noise schemes, which are independent of sampling. Recent studies have shown the key factors in training schemes influencing learning patterns and models' performance. In this sub-section, we divide the training enhancement into three categories: knowledge distillation, diffusion scheme learning, and noise scale designing.

Knowledge Distillation

Knowledge distillation is an emerging method for obtaining efficient small-scale networks by transferring "knowledge" from complex teacher models with high learning capacity to simple student models [154], [155]. Thus, student models equip the advantages in model compression and model acceleration [156], [157].

$$\theta_{stu} := \theta_{stu} - \gamma * \nabla_x [(R_{tea}(R_{tea}(x_t, t), t - 1)) - R_{stu}(x_t, t)] \quad (32)$$

Salimans *et al.* [62] first applies the core idea into diffusion model improvement by progressively distilling knowledge from one sampling model to another. In each distillation stage, student models learn to conduct two-step updates from teacher models in a one-step manner to halve their sampling steps. Unlike progressive distillation, denoising student [98] distills knowledge from scratch by minimizing KL Divergence between two categorical distributions.

Diffusion Scheme Learning

Similar to VAE, the forward diffusion process can be viewed as an encoder that projects data into many latent spaces. Thus, an effective yet expressive diffusion pattern is necessary for effective reverse decoding. Compared to VAE, the diffusion model encodes data onto latent spaces with the same dimension to achieve high expressiveness in a more complex way. Thus, we divide current methods as projecting approaches exploration and encoding degree optimization.

For encoding degree optimization methods, CCDF [95] and Franzese *et al.*, [103] establish an optimization problem where the number diffusion step is treated as a variable for minimizing ELBO from a theoretical perspective [158], [159]. Another approach is based on truncation, which conducts a trade-off between generating speed and sample fidelity. Truncating patterns samples from less diffused data generated by GAN and VAE in a one-step manner. TDPM [99] truncates both diffusion and sampling processes by sampling from implicit generative distribution learned by GAN and conditional transport (CT) [160]. Similarly, Early Stop (ES) DDPM [101] learns from latent space to generate implicit distributions.

$$\tilde{x} := R_{t^*0}(F_{0t^*}(x_0, \sigma_{0t^*}), \sigma_{t^*0}), \quad t^* \in [0, T] \quad (33)$$

For projecting approaches exploration, some works focus on the diversity of diffusion kernels. Soft diffusion [102], and blurring diffusion model [100] succeed in proving linear corruptions, including blurring and mask, can also serve as transition kernels.

Noise Scale Designing

In the traditional diffusion process, each transition step is determined by the injected noise, which is equivariant to a random walk on the forward and reversed trajectories. Thus, noise scale designing has the potential for reasonable generation and fast convergence. Unlike traditional DDPM, existing methods treat noise scale as a learnable parameter throughout the whole process.

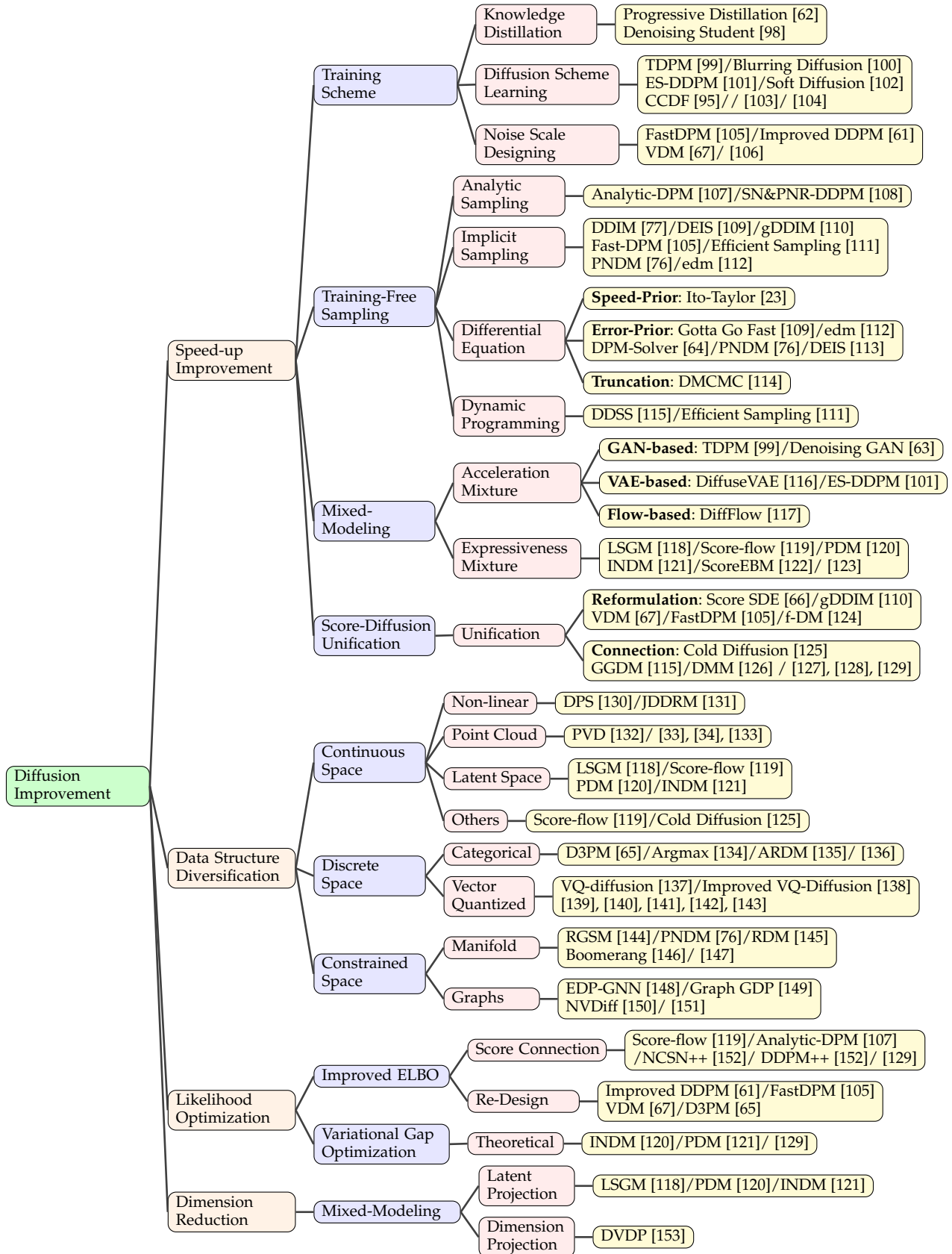
$$\begin{aligned} \text{SNR}(t) &:= \alpha_t^2 / \beta_t^2 = \exp(\gamma_\eta(t)), \quad \sigma_t^2 = \text{sigmoid}(\gamma_\eta(t)) \quad (34) \\ \mathcal{L}_T(\mathbf{x}) &= \frac{T}{2} \mathbb{E}_{\epsilon \sim \mathcal{N}(0, \mathbf{I})} [(\text{SNR}(s) - \text{SNR}(t)) \|\mathbf{x} - \hat{\mathbf{x}}_\theta(\mathbf{z}_t; t)\|_2^2] \\ \mathcal{L}_\infty(\mathbf{x}) &= \frac{1}{2} \mathbb{E}_{\epsilon \sim \mathcal{N}(0, \mathbf{I})} \int_{\text{SNR}_{\min}}^{\text{SNR}_{\max}} \|\mathbf{x} - \hat{\mathbf{x}}_\theta(\mathbf{z}_v, v)\|_2^2 dv \quad (35) \end{aligned}$$

Among the forward noise design methods, VDM [67] parameterizes the noise scalar as signal-to-noise ratio for connecting noise scale and training loss and model types. FastDPM [105] obtains forward noise from the discrete-time variables or variance scalar, connecting noise design to ELBO optimization. In the reverse noise design methods, improved DDPM [61] learns the reverse noise scale implicitly by training a hybrid loss containing L_{simple} and L_{vlb} . Besides, San Roman *et al.* employs a noise prediction network to update the reverse noise scale directly before conducting ancestral sampling in each step.

3.1.2 Training-Free Sampling

Training enhancement methods focus on changing the training pattern and noise schemes for sampling speed-up, it can also be achieved by designing advanced sampling algorithms. Based on the fact that the gradient of data is stored in the pre-trained diffusion models, training-free methods apply pre-trained information directly to the advanced sampling algorithms with fewer steps and higher fidelity, which are free from model re-training. In this subsection, we divide them into four categories: analytical methods,

TABLE 2
Classification of Improved Diffusion Techniques



implicit sampler, differential equation solver sampler, and dynamic programming adjustment.

Analytical Method

Existing training-free sampling methods take reverse covariance scales as a hand-crafted sequence of noises without considering them dynamically. Starting from KL-divergence optimization, analytical methods set the reverse mean and covariance as optimal solutions. Analytic-DPM [107] and extended Analytic-DPM [108] jointly propose optimal reverse solutions under correction for each state. Analytical methods enjoy a theoretical guarantee for the approximation error, but they are limited in particular distributions due to the pre-assumptions.

Implicit Sampler

Instead of extracting noise information step by step, the implicit sampler follows the jump-step pattern using knowledge from the pre-trained diffusion model. It follows the assumption that information from multi-step intervals can be reversed along a determinant trajectory without randomness during sampling. FastDPM [105] conducts accelerated sampling discretely by re-designing the reverse noise schedule. Song *et al.*, [77] proposes DDIM, which follows the discrete pattern of probability flow ODE with Neural ODE formulation [75]:

$$d\bar{x}(t) = \epsilon_{\theta}^{(t)} \left(\frac{\bar{x}(t)}{\sqrt{\sigma^2 + 1}} \right) d\sigma(t) \quad (36)$$

where σ_t is parameterized by $\sqrt{1 - \alpha}/\sqrt{\alpha}$, and \bar{x} is parameterized as $x/\sqrt{\alpha}$. Besides, the probability can be treated as one kind of Score SDE, which is derived from the discrete formulation:

$$\frac{x_{t-\Delta t}}{\sqrt{\alpha_{t-\Delta t}}} = \frac{x_t}{\sqrt{\alpha_t}} + \left(\sqrt{\frac{1 - \alpha_{t-\Delta t}}{\alpha_{t-\Delta t}}} - \sqrt{\frac{1 - \alpha_t}{\alpha_t}} \right) \epsilon_{\theta}^{(t)}(x_t) \quad (37)$$

Besides, the implicit sampler is actually one type of neural ODE solver. On the one hand, part of the methods employ advanced ODE solvers, such as PNDM [76], edm [112], DEIS [161], gDDIM [110], and DPM-Solver [64]. On the other hand, Watson *et al.* proposed dynamic programming based jump-step method for sampling the optimal implicit route along the reversed trajectory. Further improved works with strong theoretical support, like manifold hypothesis and sparsity, are expected.

Differential Equation Solver Sampler

Differential Equation (DE) Solver Sampler minimizes approximation error during reverse sampling with ODE/SDE-based numerical solvers [66]. With a strong assumption on the infinite-time continuous process, differential equation solvers achieve the leading performances. Generally, there are two basic DE formulations: the SDE formulation enjoys randomness when walking in the joint distribution field, ODE formulation with deterministic mapping enjoys faster speed. [23] As for the DE solvers [162], [163], higher-order DE solvers have smaller approximation errors and higher order of convergence, it requires more evaluations [164]

and suffers from instability issues. In this subsection, we introduce the current algorithms based on the trade-off of different frameworks and DE solvers. We divide them into speed-prior and accuracy-prior.

For the accuracy-prior methods, Itô-Taylor Sampling Scheme [113] has been proposed using a high-order SDE solver. Besides, ideal derivative substitution is applied to parameterize the score function in a tricky way that avoids higher-order derivative computing. For the speed-prior methods combining linear solvers and higher-order solvers, Gotta Go Fast [113] achieves an algorithm based on directional guidance on step size adjustment. edm [112] employs second-order Heun’s solver and adjusted time steps on deterministic diffusion ODE. PNDM [76] has explored that different numerical solvers can share the same gradient, leading to exploring the linear multi-step method after using three steps of a higher-order solver (Runge-Kutta method) in Diffusion ODE. Besides, DPM-solver [64] proves that a united solver cross alternative orders may perform better.

$$dx_{\pm} = -\dot{\sigma}(t)\sigma(t)\nabla_x \log p(x; \sigma(t))dt \pm \beta(t)\sigma(t)^2\nabla_x \log p(x; \sigma(t))dt + \sqrt{2\beta(t)}\sigma(t)d\omega_t, \quad (38)$$

Furthermore, from the perspective of differential equation formulation, DPM-solver, and DEIS [109] created a new viewpoint except for SDE and Diffusion ODE. The trade-off extrusion ODE can be seen as a semi-linear form by which the discretization errors are reduced. DEIS improved numerical DDIM with a multi-step PC-sampling method [161] with exponential integrator [165]. DPM-solver provided a theoretical guarantee on approximation error. Currently, semi-linear-based ODE performs the best but still requires other techniques, such as threshold limit [109] and analytical form [64].

$$\frac{dx_t}{dt} = f(t)x_t - \frac{1}{2}g^2(t)\nabla_x \log q_t(x_t) \quad (39)$$

Moreover, Denoising MCMC [114] applies truncation idea into differential equation sampling. To accelerate reverse sampling, it conducts differential sampling from data and variance generated by MCMC with a higher speed.

Dynamic Programming Adjustment

Dynamic programming (DP) achieves the traversal of all choices to find the optimized solution in a reduced time by memorization technique [166], [167]. Assuming that each path from one state to another state shares the same KL divergence with others, dynamic programming algorithms explore the optimal traversal along the trajectory. Current DP-based methods [111], [168] take $\mathcal{O}(T^2)$ of computational cost via optimizing the sum of ELBO losses.

3.1.3 Mixed-Modeling

Mixed-modeling applies fast-sampling, and high-expressiveness generative models in diffusion pipeline [169], [170], [171], [172]. For diffusion mixed-modeling, diffusion models take the virtue of high-speed sampling of others (such as adversarial training network and autoregressive encoder) and high expressiveness (such as

normalizing flow). Thus, designing mixed models not only performs a promising enhancement but also helps perceive connections between diffusion models and others. Mixed modeling improvement can be classified into two classes from the perspective of mixing purposes: acceleration mixture and expressiveness mixture.

Acceleration Mixture

Acceleration mixture aims at applying high-speed generation of VAEs and GANs to save plenty of steps on sampling less perturbed data from random noise. One type of models generate predicted x'_0 with VAE [116] and GAN [63]. Another type of model like ES-DDPM [101] reconstructs intermediate samples as the starting points of the denoised process, which can be viewed as the early stop technique.

$$x_{t-1} := R_t(x_t, \sigma_t | \tilde{x}), \quad \tilde{x} := \text{Dec}(\text{Enc}(x_0)) \quad (40)$$

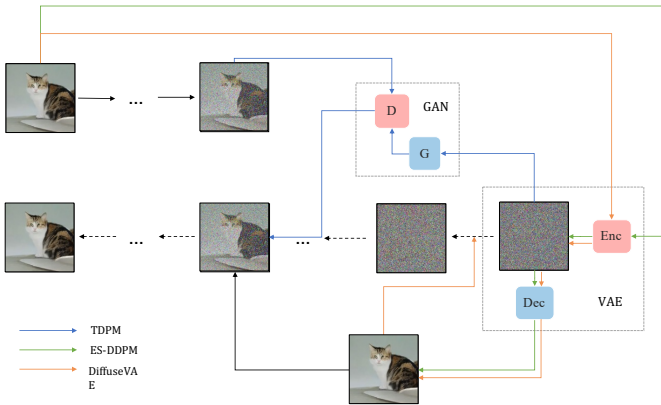


Fig. 4. Acceleration mixed-modeling pipeline. The blue line represents the pipeline of TDPM. The partly perturbed data x_t is applied as the ground-truth condition for GAN’s generator, and the conditional samples x'_t with the same perturbation level are generated from the latent before being compared with x_t . The successful samples are applied as the beginning of the reverse process. Instead of using GAN as the high-speed generator, ES-DDPM follows the pattern of TDPM’s with VAE, shown with green lines. Besides, DiffuseVAE employs VAE to generate condition \tilde{x}_0 in each sampling step.

Expressiveness Mixture

Expressiveness mixture support diffusion models on expressing data or noise in a different pattern. High-expressiveness data combined with fast-sampling generative models achieve speed-up by obtaining mean and variance more accurately. The high expressiveness methods can be divided into noise modulation, space projection, and kernel expressiveness. As for noise modulation, DiffFlow [117] employs a flow function in each SDE-based diffusion step for noise modulation through a minimizing process w.r.t. KL-Divergence. Benefiting from specific spaces’ properties, space projection methods leverage NFs into data transformation. Both LSGM [118], and PDM [120] obtained latent variables using VAE and flow function, respectively, to take advantage of fast computing. Besides, Score-Flow [119] conducts the diffusion process onto the dequantization field using NFs to solve the mismatching between continuous density and discrete data [173]. By taking the energy function as the transition kernel in the reverse process, kernel expressiveness method [122], [174] bridges the

gap between non-normalized probability density data and diffusion sampling.

$$\tilde{x} := f_\phi^{-1}(R_{T_0}(F_{0T}(f_\phi(x_0), \sigma_{0T}), \sigma_{T_0})) \quad (41)$$

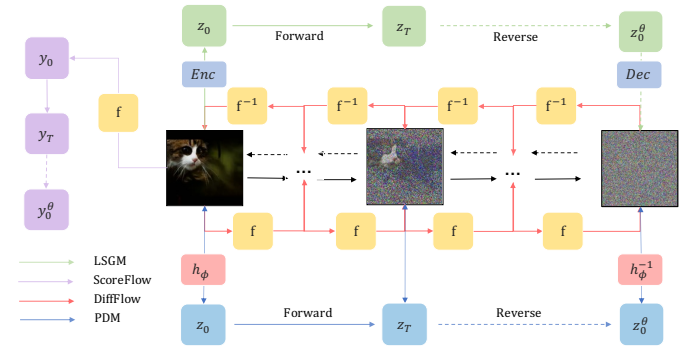


Fig. 5. Expressiveness mixed-modeling pipeline. The models for expressiveness enhancement keep the same procedure as DDPM in the training, diffusion, and sampling process, denoted by black lines. Furthermore, additional improvements are highlighted by other colors. The red lines show the pipeline of DiffFlow, which adds a flow function and related inverse function at each step. The works in blue and green lines represent the idea of latent space diffusion by jointly training mixture models. Different supporting generative models are used in LSGM and PDM. Besides, Score-Flow uses the flow function as a projector from discrete to dequantization space. Then generating dequantized samples using the traditional diffusion method.

3.1.4 Score & Diffusion Unification

ScoreSDE [66] first contributed to score & diffusion unification. It builds a unified continuous framework, linking diffusion and perturbation processes to provide a universal tool for generation tasks. Score-diffusion unification models work because the insight from landmark unification helps in exploring efficient sampling mechanisms. Furthermore, generalized works provide multi-view for benefiting diffusion models. There are two categories of works: diffusion reformulation works and diffusion & score connection works.

Reformulation problems unify diffusion pipeline based on one or two variables (such as time t and signal-to-noise ratio). FastDPM [105], VDM [67], and f-DM [124] unify DDPM w.r.t. noise schedules by the noise-time bijective map, signal-to-noise ratio, and signal transformation. Generalized DDIM (gDDIM) [110] unifies the DDIM family according to the transition kernel during each step, benefiting implicit acceleration from the bottom. With lighter reparameterization, the methods usually enjoy simplified training and controllable sampling through prejudice optimization. Furthermore, generalized frameworks support exploration of new diffusion pattern.

Connection problems link the score and diffusion frameworks to extend them into a higher view. Gong *et al.*, [127] reveals the hidden connection between score matching with the normalizing flow, expressing score matching by flow ODEs [75], [175]. Bortoli *et al.*, [128] presents a variational score matching approach for simulating diffusion bridges using Doob-h transformation [176]. GGDM [111] and DMM [126] generalizes diffusion models with non-Markovian samplers and a vast range of marginal variance to explore formulations of a wider diffusion family. Cold Diffusion

[125] proposes a unified training and inference framework available for any transition kernels and data distributions. Huang *et al.* [129] presents a variational form for likelihood estimation, enhancing theoretical support for variational gap minimization. Viewing diffusion model with less pre-assumption, more fundamental setting can be solved and explained.

3.2 Data Structure Diversification

Diffusion methods are mostly conducted on image generation tasks, which limits the high-fidelity generation potential on applications in the other fields. until now, diffusion mechanism is proved to work in inter-disciplinary tasks with diverse data types [48], [55]. More importantly, the traditional patterns of diffusion based on Gaussian perturbed kernels and Gaussian noise prior are expected to be extended for universal practices. To improve diffusion model’s generalization power, we divided the distribution diversification into three aspects: discrete space, continuous space, and Constrained space with structural constraints.

3.2.1 Continuous Space

Non-linear Space

While existing denoising and super-resolution methods handle linear perturbation, non-linear space has great effects on low-level vision tasks such as phase retrieval and non-uniform deblurring. Kawar *et al.*, [131] and DPS [130] apply pseudo-inverse operator and posterior sampling approximation into non-linear noise prediction to solve JPEG artifact correction, image deblurring, and phase retrieval.

Image & Point Cloud

Point cloud generation is first proposed by Luo *et al.* [33], which generates latent samples for point cloud data, and conducts transformation to obtain high-quality 3d shapes. Other techniques such as [34], [132], [133] accomplish the shape generation and completion tasks similarly. Some slight improvements used in latent space transformation such as canonical map [133], condition feature extraction sub-nets [34], and point-voxel representation [132].

Latent Space

Similar to Expressiveness mixture modeling, latent space data distributions are often processed for diffusion application since different types of complex data structures require a unified approach to generalize and analyze. Most current methods project data into continuous space, obtaining promising performance with the aid of high-quality generation power of diffusion models such as EDM [21] and antigen-diffusion [22]. Thus, latent space processing should be a beneficial pattern utilized in new application fields.

Function

Traditional diffusion processes conducted by Gaussian distribution are limited for some real-world tasks, which leads to continuous function probabilistic modeling. Dutordoir *et al.*, [177] proposes the first diffusion model sampling on the function space. It captures the multi-dimensional distributions by sampling from joint posteriors.

Others

Score-flow [119] employs a flow function to project RGB-image into dequantization space, achieving diffusion techniques for generating accurate samples. Cold diffusion [125] proposes algorithms for projecting data into random distributions with the support of reconstructing correction.

3.2.2 Discrete Space

Deep generative models have many significant achievements in natural language processing [178], [179], multi-modal learning [85], [180], and AI for science [181], [182] with relevant architectures and advanced techniques. Among these successes, processing discrete data such as sentences, residue, atom, and vector-quantized data is necessary for eliminating inductive bias. So, based on the previous fortune, it seems that conducting relevant tasks with diffusion models is promising foreground. We divide the main problem into processing text & categorical data, and vector-quantized data.

Text & Categorical

To process categorical features, D3PM [65] first promoted diffusion algorithm onto discrete space to deal with discrete data like sentences and images employing defining w.r.t. categorical distribution $\text{Cat}()$:

$$q(x_t | x_{t-1}) = \text{Cat}(x_t; p = x_{t-1} \mathbf{Q}_t) \quad (42)$$

Similar to D3PM, multi-nomial diffusion [134] and ARDM [135] extended the categorical diffusion into multi-nomial data for generating language text & segmentation map and Lossless Compression.

Vector-Quantized

To handle the multi-model problem such as text-to-image generation, text-to-3d generation, and text-to-image editing, vector-quantized (VQ) data is proposed to combine data from different fields into the codebook. VQ data processing achieved great performance in autoregressive encoders [183]. Gu *et al.* [137] first applied diffusion techniques into VQ data, solving unidirectional bias as well as accumulation prediction error problems existing in VQ-VAE. Further text-to-image works such as Cohen *et al.* [139] & Improved VQ-Diffusion [138], text-to-pose works such as Xie *et al.* [140] & Guo *et al.* [141], and text-to-multimodal works such as Weinbach *et al.* [142] & Xu *et al.* [143] are built on this core idea. The transition process driven by the probability transition matrix \mathbf{Q} and categorical representation vector \mathbf{v} is defined by

$$q(x_t | x_{t-1}) = \mathbf{v}^\top(x_t) \mathbf{Q}_t \mathbf{v}(x_{t-1}) \quad (43)$$

$$\mathbf{Q}_t = \begin{bmatrix} \alpha_t + \beta_t & \beta_t & \beta_t & \cdots & 0 \\ \beta_t & \alpha_t + \beta_t & \beta_t & \cdots & 0 \\ \beta_t & \beta_t & \alpha_t + \beta_t & \cdots & 0 \\ \vdots & \vdots & \vdots & \ddots & \vdots \\ \gamma_t & \gamma_t & \gamma_t & \cdots & 1 \end{bmatrix} \quad (44)$$

3.2.3 Constrained Space

Graph-based neural networks step over traditional data constraints and re-express latent connections among existing data such as social networks [184], [185], molecular [186], [187], and weather conditions [188], [189]. Moreover, manifold learning methods hold the advantages of non-redundant expression and comprehensive portrayals, such as protein and RNA. Thus, constrained space extension methods are based on the Riemann manifold and graph.

Manifold Space

Most current data structures, such as images and video, are defined in a flat-geometry manifold (Euclidean space). However, there exists a series of data in the field of robotics [190], geoscience [191], and protein modeling [192] defined in Riemannian manifold [193], where current methods for Euclidean space cannot capture the high-dimensional Riemann feature. Thus, recent methods RDM [145], RGSM [144], and Boomerang [146] applied diffusion sampling into the Riemannian manifold based on score SDE framework [66]. Besides, there are relevant theoretical works [76], [147] providing comprehensive support for manifold sampling.

Graph

According to [194], graph-based neural networks are becoming an increasingly popular trend due to the high expressiveness in the human pose [141], molecules [195], and proteins [57]. Many current methods apply diffusion theories to graph space. In EDP-GNN [148], Pan *et al.* [151], and GraphGDP [149], graph data is processed through adjacency matrices for capturing the graph’s permutation invariance. NVDiff [150] reconstructs node positions by reverse SDE.

3.3 Likelihood Optimization

Most variational methods [183], [196] and diffusion methods [68] train models by the principle of variational evidence lower bound (ELBO) since the log-likelihood is not tractable. However, sometimes the log-likelihood still needs to be competitive because the variational gap between ELBO and log-likelihood is not minimized simultaneously. Thus, several methods [61], [119] directly focus on the likelihood optimization problem to solve this problem. And, the solutions can be classified into two classes – improved ELBO and variational gap optimization.

3.3.1 Improved ELBO

Score Connection

Inspired by [197], [198], score connection methods provide a new connection between ELBO optimization and score matching, solving the likelihood optimization problems via improved score training. Score-flow [119] treats the forward KL divergence in ELBO as optimizing a score-matching loss with a weighted scheme. Huang *et al.* [129] treated Brownian motion as a latent variable to track the log-likelihood estimation explicitly, and it builds the bridge between the estimation and weighted score matching in the variational framework. Analytic-DPM [107] enhances ELBO by analyzing the KL Divergence and reverse covariance & mean. Similarly, NCSN++ [152] bridges the theoretical gap by introducing a truncation factor to ELBO.

$$\mathcal{E}^\infty := \mathbb{E}\left[-\frac{1}{2} \int_0^T \|a(\omega, s)\|_2^2 ds + \log p_0(x_T) - \int_0^T \nabla \cdot \mu ds \mid x_0 = x\right] \quad (45)$$

Re-Design

Compared to loss transformation techniques, re-Design methods directly tighten the ELBO by re-designing noise scale and training objectives. VDM [67] and DDPM++ [152] connect the advanced training objectives concerning signal-to-noise ratio and truncate factors, respectively, optimizing ELBO via finding optimal factors. Improved DDPM [61] and D3PM [65] propose hybrid loss functions based on ELBO with a weighted scheme for improving ELBO.

$$L_{\text{hybrid}} = L_{\text{simple}} + \lambda L_{\text{vlb}} \quad (46)$$

3.3.2 Variational Gap Optimization

Apart from designing advanced ELBO, minimizing the variational gap is still one approach to maximize the log-likelihood. Based on the success of variational gap optimization [199] in the VAE field, INDM [120] applies the flow model to express the variational gap, minimizing the gap by jointly training the bidirectional flow model and linear diffusion model on latent space. Additionally, PDM accomplishes the variational gap expression by introducing encoder loss of VAE. With collective training, a unique optimal solution exists to eliminate the gap.

$$L_{vb}^* := L_{h_\phi} + L_{vb} \left(\left\{ \mathbf{z}_t^\phi \right\}_{t=0}^T; \theta \right) + L_0 \left(\left\{ \mathbf{z}_t^\phi \right\}_{t=0}^T; \theta \right) \quad (47)$$

3.4 Dimension Reduction

Unlike the variational auto-encoder that projects data into the latent lower dimension, inferencing on the high-dimensional dataset is extremely consuming. However, diffusion models enjoy high expressiveness from equal-dimension transitions considering that dimension reduction may cause the information to be missing. Actually, diffusing on the low-dimensional manifold has wide applications in graph-based representations. Thankfully, reduced-dimension diffusion can be achieved with the aid of latent projection and dimension projection techniques.

Latent Projection

Several mix-modeling methods project training data onto the latent space with a lower dimension by flow function and VAE-encoder, conducting diffusion and denoising processes. LSGM [118], INDM [121], and PDM [120] follow the pattern to learn smoother models in a smaller space, triggering fewer network evaluations and faster sampling [118]. Furthermore, weighting training techniques that use joint training of both diffusion models and projecting models based on ELBO maximization and log-likelihood maximization are employed.

$$L := L_{Enc}(z_0|x) + L_{Dec}(x|z_0) + L_{simple} \left(\left(\left\{ \mathbf{z}_t^\theta \right\}_{t=0}^T \right); \theta \right), \quad (48)$$

Dimension Projection

Dimension projection aims to clear spatial redundancy on image manifolds by decomposing the invertible signal by multiple orthogonal ones. DVDP [153] conducts subspace inference during perturbation and reconstruction, which can be seen as a mixture of DDPM and VAE. Besides, the theoretical analysis behind the reduction scale of dimensionality and down-sampling & up-sampling steps are worth to be explored.

4 APPLICATION

Benefiting from the powerful ability to generate realistic samples, diffusion models have been widely used in various fields such as computer vision [200], natural language processing, and bioinformatics.

4.1 Computer vision

4.1.1 Low-level vision

CMDE [27] empirically compared score-based diffusion methods in modeling conditional distributions of visual image data and introduced a multi-speed diffusion framework. By leveraging the controllable diffusion speed of the condition, CMDE outperformed the vanilla conditional denoising estimator [69] in terms of FID scores in in-painting and super-resolution tasks. DDRM [201] proposed an efficient, unsupervised posterior sampling method served for image restoration. Motivated by variational inference, DDRM demonstrated successful applications in super-resolution, deblurring, inpainting, and colorization of diffusion models. Palette [97] further developed a unified diffusion-based framework for low-level vision tasks such as colorization, inpainting, cropping, and restoration. With its simple and general idea, this work demonstrated the superior performance of diffusion models compared to GAN models. DiffC [202] proposed an unconditional generative approach that encoded and denoise corrupted pixels with a single diffusion model, which showed the potential of diffusion models in lossy image compression. SRDiff [29] exploited the diffusion-based single-image super-resolution model and showed competitive results. RePaint [203] was a free-form inpainting method that directly employed a pre-trained diffusion model as the generative prior and only replaced the reverse diffusion by sampling the unmasked regions using the given image information. Though there was no modification to the vanilla pre-trained diffusion model, this method was able to outperform autoregressive and GAN methods under extreme tasks.

4.1.2 High-level vision

FSDM [30] was a few-shot generation framework based on conditional diffusion models. Leveraging advances in vision transformers and diffusion models, FSDM can adapt quickly to various generative processes at test-time and performs well under few-shot generation with strong transfer capability. CARD [31] proposed classification and regression diffusion models, combining a denoising diffusion-based conditional generative model and a pre-trained conditional mean estimator to predict data distribution under given conditions. Though approaching supervised learning from a conditional generation perspective and training with objectives

indirectly related to the evaluation metrics, CARD presented a strong ability in uncertainty estimation with the help of diffusion models. Motivated by CLIP [204], GLIDE [85] explored realistic image synthesis conditioned on the text and found that diffusion models with classifier-free guidance yielded high-quality images containing a wide range of learned knowledge. DreamFusion [205] extends GLIDE's achievement into 3D space. To obtain expressive generative models within a smooth and limited space, LSGM [118] built a diffusion model trained in the latent space with the help of a variational autoencoder framework. SegDiff [206] extended diffusion models for performing image-level segmentation by summing up feature maps from a diffusion-based probabilistic encoder and an image feature encoder. Video diffusion [26], on the other hand, extended diffusion models in the time axis and performed video-level generation by utilizing a typically designed reconstruction-guided conditional sampling method. VQ-Diffusion [32] improved vanilla vector quantized diffusion by exploring classifier-free guidance sampling for discrete diffusion models and presenting a high-quality inference strategy. This method showed superior performance on large datasets such as ImageNet [207] and MSCOCO [208]. Diff-SCM [209] built a deep structural model based on the generative diffusion model. It achieved counterfactual estimation by inferring latent variables with deterministic forward diffusion and intervening in the backward process.

4.1.3 3D vision

[33] was an early work on diffusion-based 3D vision tasks. Motivated by the non-equilibrium thermodynamics, this work analogized points in point clouds as particles in a thermodynamic system and employed the diffusion process in point cloud generation, which achieved competitive performance. PVD [210] was a concurrent work on diffusion-based point cloud generation but performed unconditional generation without additional shape encoders, while a hybrid and point-voxel representation was employed for processing shapes. PDR [34] proposed a paradigm for diffusion-based point cloud completion that applied a diffusion model to generate a coarse completion based on the partial observation and refined the generated output by another network. To deal with point cloud denoising, [35] introduced a neural network to estimate the score of the distribution and denoised point clouds by gradient ascent.

4.1.4 Video modeling

Video diffusion [26] introduced the advances in diffusion-based generative models into the video domain. RVD [211] employed diffusion models to generate a residual to a deterministic next-frame prediction conditioned on the context vector. FDM [212] applied diffusion models to assist long video prediction and performed photo-realistic videos. MCVD [36] proposed a conditional video diffusion framework for video prediction and interpolation based on masking frames in a blockwise manner. RaMViD [37] extended image diffusion models to videos with 3D convolutional neural networks and designed a conditioning technique for video prediction, infilling, and upsampling.

4.1.5 Medical application

It is a natural choice to apply diffusion models to medical images. Score-MRI [38] proposed a diffusion-based framework to solve magnetic resonance imaging (MRI) reconstruction. [213] was a concurrent work but provided a more flexible framework that did not require a paired dataset for training. With a diffusion model trained on medical images, this work leveraged the physical measurement process and focused on sampling algorithms to create image samples that are consistent with the observed measurements and the estimated data prior. R2D2+ [214] combined diffusion-based MRI reconstruction and super-resolution into the same network for end-to-end high-quality medical image generation. [215] explored the application of the generative diffusion model to medical image segmentation and performed counterfactual diffusion.

4.2 Sequential modeling

4.2.1 Natural language processing

Benefited by the non-autoregressive mechanism of diffusion models, Diffusion-LM [39] took advantage of continuous diffusions to iteratively denoise noisy vectors into word vectors and performed controllable text generation tasks. Bit Diffusion [40] proposed a diffusion model for generating discrete data and was applied to image caption tasks.

4.2.2 Time series

To deal with time series imputation, CSDI [41] utilized score-based diffusion models conditioned on observed data. Inspired by masked language modeling, a self-supervised training procedure was developed that separates observed values into conditional information and imputation targets. SSSD [42] further introduced structured state space models to capture long-term dependencies in time series data. CSDE [254] proposed a probabilistic framework to model stochastic dynamics and introduced Markov dynamic programming and multi-conditional forward-backward losses to generate complex time series.

4.3 Audio

WaveGrad [43] and DiffWave [44] were seminal works that applied diffusion models to raw waveform generation and obtained superior performance. GradTTS [45] and DiffTTS [265] also implemented diffusion models but generated mel feature instead of raw waves. DiffVC [264] further challenged the one-shot many-to-many voice conversion problem and developed a stochastic differential equation solver. DiffSinger [46] extended the common sound generation to singing voice synthesis based on a shallow diffusion mechanism. DiffSound [259] proposed a sound generation framework conditioned on the text that employed a discrete diffusion model to replace the autoregressive decoder to overcome the unidirectional bias and accumulated errors. EdiTTS [47] was also a diffusion-based audio model for the text-to-speech task. Through coarse perturbations in the prior space, desired edits were induced during denoising reversal. Guided-TTS [48] and Guided-TTS2 [49] were also an early series of text-to-speech models that successfully applied diffusion models in sound generation.

[266] combined a voice diffusion model with a spectrogram-domain conditioning method and performed text-to-speech with voices unseen during training. InferGrad [267] considered the inference process in training and improved the diffusion-based text-to-speech model when the number of inference steps is small, enabling fast and high-quality sampling. SpecGrad [50] brought ideas from signal processing and adapted the time-varying spectral envelope of diffusion noise based on the conditioning log-mel spectrogram. ItôTTS [24] unified text-to-speech and vocoder into a framework based on linear SDE. ProDiff [32] proposed a progressive and fast diffusion model for high-quality text-to-speech. Instead of hundreds of iterations, ProDiff parameterized the model by predicting clean data and employed a teacher-synthesized mel-spectrogram as a target to reduce data discrepancies and make a sharp prediction. Binaural-Grad [260] was a two-stage diffusion-based framework that explored the application of diffusion models in binaural audio synthesis given mono audio.

4.4 AI for science

4.4.1 Molecular conformation generation

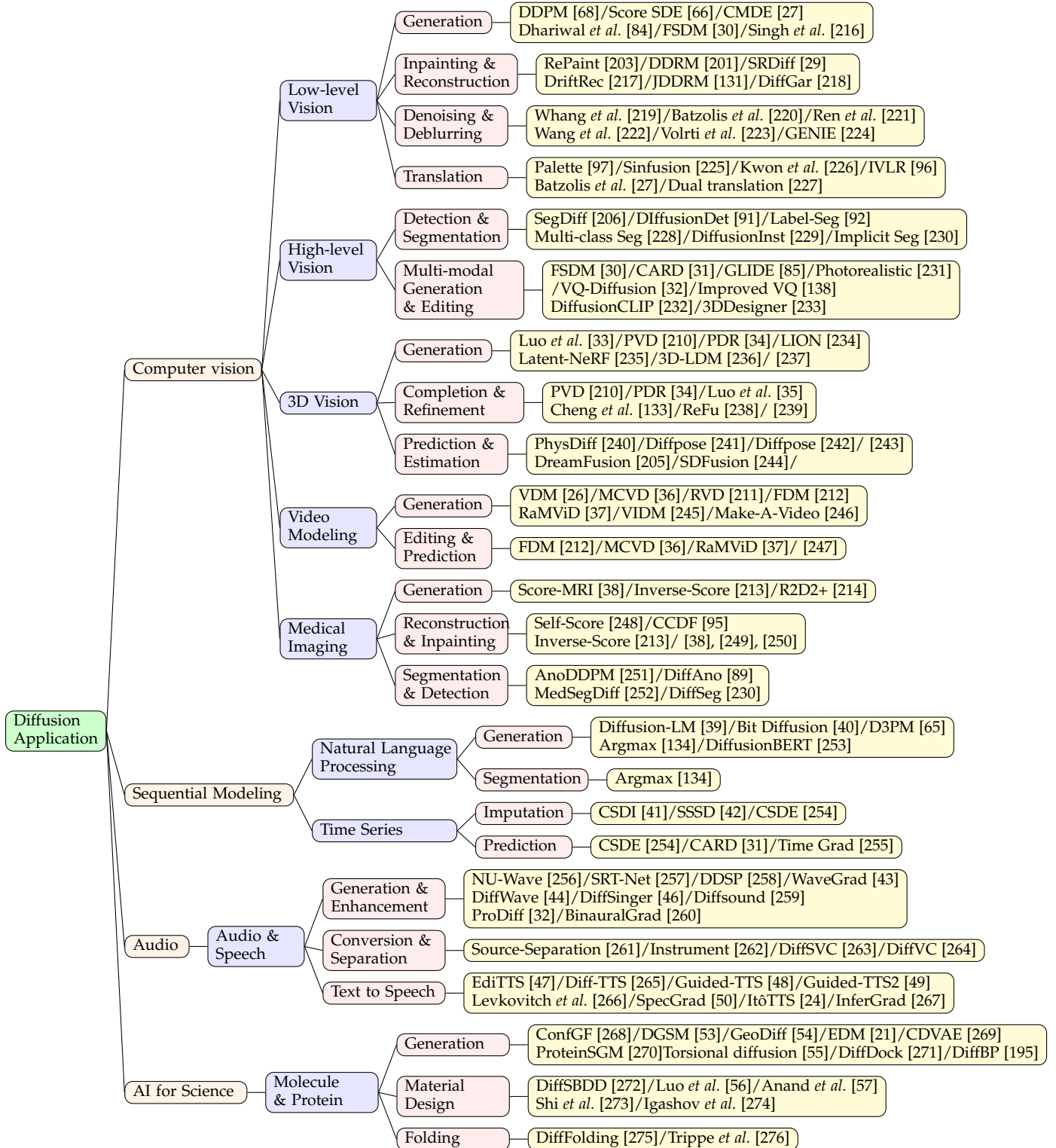
ConfGF [268] was an early work on diffusion-based molecular conformation generation models. While preserving rotation and translation equivariance, ConfGF generated samples by Langevin dynamics with physically inspired gradient fields. However, ConfGF only modeled local distances between the first-order, the second-order, and the third-order neighbors and thus failed to capture long-range interactions between non-bounded atoms. To tackle this challenge, DGSM [53] proposed to dynamically construct molecular graph structures between atoms based on their spatial proximity. GeoDiff [54] found that the model was fed with perturbed distance matrices during diffusion learning, which might violate mathematical constraints. Thus, GeoDiff introduced a roto-translational invariant Markov process to impose constraints on the density. EDM [21] further extended the above methods by incorporating discrete atom features and deriving the equations required for log-likelihood computation. Torsional diffusion [55] operated on the space of torsional angles and produced molecular conformations according to a diffusion process limited to the most flexible degrees of freedom. Based on previous geometric deep learning methods, DiffDock [271] conducts denoised score matching on transition, rotation, and torsion angle to generate drug conformation in protein-ligand complexes.

4.4.2 Material design

CDVAE [269] explored the periodic structure of stable material generation. To address the challenge that stable materials exist only in a low-dimensional subspace with all possible periodic arrangements of atoms, CDVAE designed a diffusion-based network as a decoder with output gradients leading to local minima of energy and updated atom types to capture specific local bonding preferences depending on the neighbors.

Inspired by the recent success of antibody modeling [277], [278], [279], the recent work [56] developed

TABLE 3
Classification of Diffusion-based model Applications



a diffusion-based generative model that explicitly targeted specific antigen structures and generated antibodies. The proposed method jointly sampled antibody sequences and structures and iteratively generated candidates in the sequence-structure space.

Anand *et al.* [57] introduced a diffusion-based generative model for both protein structure and sequence and learned the structural information that is equivariant to rotations and translations. ProteinSGM [270] formulated protein design as an image inpainting problem and applied conditional diffusion-based generation to precisely model the protein structure. DiffFolding [275] generates protein backbone concentrating on internal angles by traditional DDPM idea.

5 CONCLUSIONS & DISCUSSIONS

The diffusion model becomes increasingly crucial to a wide range of applied fields. To utilize the power of the diffusion model, this paper provides a comprehensive and up-to-date review of several aspects of diffusion models using detailed insights on various attitudes, including theory, improved algorithms, and applications. We hope this survey serves as a guide for readers on diffusion model enhancement and its application.

6 LIMITATIONS & FURTHER DIRECTIONS

Attention on diffusion model class: Most existing improvements and application algorithms are based on the original setting as DDPM. However, many aspects are ignored by researchers concerning the generalized setting of diffusion-based models. Further meaningful works that explore prior distribution, transition kernel, sampling algorithm, and diffusion schemes are expected. Diffusion models should be viewed as a class, but not a branch of DDPM-based models.

Training objective & evaluation metric: Most diffusion-based models set training objectives as evidence of lower bound (ELBO) of negative log-likelihood. However, we have no clear theory that ELBO and NLL are optimized simultaneously. Therefore, the inconsistency may lead to a hidden mismatch between the real goal and the practical refinement of designing. Consequently, further analytical approaches linking log-likelihood optimization to existing variables or creating novel training objectives consistent with the likelihood may guide a significant enhancement of the model's performance. Furthermore, current evaluation metrics like FID and IS scores cannot perfectly match the primary goals since data distributions are not equivariant to likelihood matching. The ideal evaluation metric should test the sample diversity as well as the recovery effect of diffusion models. A diversity score considering enough classes like CLIP [204] may be an available solution. A recovery score considering real-world data on the manifold for distribution distance will describe the model's generating ability more accurately and comprehensively. To sum up, the training objective and evaluation metric need to follow the initial goal.

Application and inductive bias: Various fields such as AI for science and natural language processing achieve

significant progress with the aid of generative models but require complex modeling to eliminate the inductive bias. There is a range of tasks that still require refinement with diffusion models to obtain better performance than existing generative networks. For current tasks based on diffusion models, the corresponding frameworks are dominated by score-based networks and DDPM. Accordingly, improvement algorithms with reduced steps should draw much attention, which is one of our motivations for this survey.

ACKNOWLEDGMENTS

This work is supported by the Science and Technology Innovation 2030 - Major Project (No. 2021ZD0150100) and the National Natural Science Foundation of China (No. U21A20427).

We appreciate Dr. Jindong Wang provided the idea for our classification figures.

REFERENCES

- [1] D. J. Rezende, S. Mohamed, and D. Wierstra, "Stochastic back-propagation and approximate inference in deep generative models," in *ICML*, 2014. (document)
- [2] C. Doersch, "Tutorial on variational autoencoders," *arXiv preprint arXiv:1606.05908*, 2016. (document)
- [3] D. P. Kingma, M. Welling *et al.*, "An introduction to variational autoencoders," *Foundations and Trends® in Machine Learning*, 2019. (document)
- [4] A. Oussidi and A. Elhassouny, "Deep generative models: Survey," in *ISCV*. IEEE, 2018. (document)
- [5] Y. LeCun, S. Chopra, R. Hadsell, M. Ranzato, and F. Huang, "A tutorial on energy-based learning," *Predicting structured data*, 2006. (document)
- [6] J. Ngiam, Z. Chen, P. W. Koh, and A. Y. Ng, "Learning deep energy models," in *ICML*, 2011. (document)
- [7] A. G. ALIAS PARTH GOYAL, N. R. Ke, S. Ganguli, and Y. Bengio, "Variational walkback: Learning a transition operator as a stochastic recurrent net," *NIPS*, vol. 30, 2017. (document)
- [8] T. Kim and Y. Bengio, "Deep directed generative models with energy-based probability estimation," *arXiv preprint arXiv:1606.03439*, 2016. (document)
- [9] I. Goodfellow, J. Pouget-Abadie, M. Mirza, B. Xu, D. Warde-Farley, S. Ozair, A. Courville, and Y. Bengio, "Generative adversarial networks," *Communications of the ACM*, 2020. (document)
- [10] A. Creswell, T. White, V. Dumoulin, K. Arulkumaran, B. Sengupta, and A. A. Bharath, "Generative adversarial networks: An overview," *IEEE Signal Process*, 2018. (document)
- [11] J. Gui, Z. Sun, Y. Wen, D. Tao, and J. Ye, "A review on generative adversarial networks: Algorithms, theory, and applications," *IEEE TKDE*, 2021. (document)
- [12] M. Mirza and S. Osindero, "Conditional generative adversarial nets," *arXiv preprint arXiv:1411.1784*, 2014. (document)
- [13] M. Arjovsky, S. Chintala, and L. Bottou, "Wasserstein generative adversarial networks," in *ICML*, 2017. (document)
- [14] L. Dinh, J. Sohl-Dickstein, and S. Bengio, "Density estimation using real nvp," *arXiv preprint arXiv:1605.08803*, 2016. (document)
- [15] D. Rezende and S. Mohamed, "Variational inference with normalizing flows," in *ICML*, 2015. (document)
- [16] I. Kobyzev, S. J. Prince, and M. A. Brubaker, "Normalizing flows: An introduction and review of current methods," *IEEE TPAMI*, 2020. (document)
- [17] S. Bond-Taylor, A. Leach, Y. Long, and C. Willcocks, "Deep generative modelling: A comparative review of vaes, gans, normalizing flows, energy-based and autoregressive models." *IEEE TPAMI*, 2021. (document)
- [18] G. Papamakarios, E. T. Nalisnick, D. J. Rezende, S. Mohamed, and B. Lakshminarayanan, "Normalizing flows for probabilistic modeling and inference." *J. Mach. Learn. Res.*, vol. 22, no. 57, pp. 1–64, 2021. (document), 1
- [19] C. Winkler, D. Worrall, E. Hoogeboom, and M. Welling, "Learning likelihoods with conditional normalizing flows," *arXiv preprint arXiv:1912.00042*, 2019. (document)

- [20] C. Saharia, W. Chan, H. Chang, C. A. Lee, J. Ho, T. Salimans, D. J. Fleet, and M. Norouzi, "Palette: Image-to-image diffusion models," 2021. [Online]. Available: <https://arxiv.org/abs/2111.05826> (document)
- [21] E. Hoogeboom, V. G. Satorras, C. Vignac, and M. Welling, "Equivariant diffusion for molecule generation in 3d," in *ICML*. PMLR, 2022, pp. 8867–8887. (document), 3.2.1, 4.4.1, 3, 9
- [22] S. Luo, Y. Su, X. Peng, S. Wang, J. Peng, and J. Ma, "Antigen-specific antibody design and optimization with diffusion-based generative models," *bioRxiv*, 2022. [Online]. Available: <https://www.biorxiv.org/content/early/2022/07/11/2022.07.10.499510> (document), 3.2.1
- [23] H. Tachibana, M. Go, M. Inahara, Y. Katayama, and Y. Watanabe, "It^o-taylor sampling scheme for denoising diffusion probabilistic models using ideal derivatives," *arXiv preprint arXiv:2112.13339*, 2021. (document), 2, 3.1.2, 8
- [24] S. Wu and Z. Shi, "It^ots and it^owave: Linear stochastic differential equation is all you need for audio generation," *arXiv e-prints*, pp. arXiv-2105, 2021. (document), 4.3, 3, 9
- [25] J. Sohl-Dickstein, E. Weiss, N. Maheswaranathan, and S. Ganguli, "Deep unsupervised learning using nonequilibrium thermodynamics," in *International Conference on Machine Learning*. PMLR, 2015, pp. 2256–2265. (document), 2.1.4, 8
- [26] J. Ho, T. Salimans, A. Gritsenko, W. Chan, M. Norouzi, and D. J. Fleet, "Video diffusion models," 2022. (document), 2.4.2, 4.1.2, 4.1.4, 3, 9
- [27] G. Batzolis, J. Stanczuk, C.-B. Schönlieb, and C. Etmann, "Conditional image generation with score-based diffusion models," *arXiv preprint arXiv:2111.13606*, 2021. (document), 4.1.1, 3, 9
- [28] L. Theis, A. van den Oord, and M. Bethge, "A note on the evaluation of generative models," in *ICLR*, 2016, pp. 1–10. (document)
- [29] H. Li, Y. Yang, M. Chang, S. Chen, H. Feng, Z. Xu, Q. Li, and Y. Chen, "Srdiff: Single image super-resolution with diffusion probabilistic models," *Neurocomputing*, 2022. (document), 4.1.1, 3, 9
- [30] G. Giannone, D. Nielsen, and O. Winther, "Few-shot diffusion models," *arXiv preprint arXiv:2205.15463*, 2022. (document), 4.1.2, 3, 9
- [31] X. Han, H. Zheng, and M. Zhou, "Card: Classification and regression diffusion models," *arXiv preprint arXiv:2206.07275*, 2022. (document), 4.1.2, 3, 9
- [32] R. Huang, Z. Zhao, H. Liu, J. Liu, C. Cui, and Y. Ren, "Prodiff: Progressive fast diffusion model for high-quality text-to-speech," *arXiv preprint arXiv:2207.06389*, 2022. (document), 4.1.2, 4.3, 3, 9
- [33] S. Luo and W. Hu, "Diffusion probabilistic models for 3d point cloud generation," in *CVPR*, 2021, pp. 2837–2845. (document), 2, 3.2.1, 4.1.3, 3, 8, 9
- [34] Z. Lyu, Z. Kong, X. Xu, L. Pan, and D. Lin, "A conditional point diffusion-refinement paradigm for 3d point cloud completion," *arXiv preprint arXiv:2112.03530*, 2021. (document), 2, 3.2.1, 4.1.3, 3, 8, 9
- [35] S. Luo and W. Hu, "Score-based point cloud denoising," in *ICCV*, 2021, pp. 4583–4592. (document), 4.1.3, 3, 9
- [36] V. Voleti, A. Jolicoeur-Martineau, and C. Pal, "Mcvd: Masked conditional video diffusion for prediction, generation, and interpolation," *arXiv preprint arXiv:2205.09853*, 2022. (document), 4.1.4, 3, 9
- [37] T. Höpfe, A. Mehrjou, S. Bauer, D. Nielsen, and A. Dittadi, "Diffusion models for video prediction and infilling," *arXiv preprint arXiv:2206.07696*, 2022. (document), 4.1.4, 3, 9
- [38] H. Chung and J. C. Ye, "Score-based diffusion models for accelerated mri," *Medical Image Analysis*, p. 102479, 2022. (document), 4.1.5, 3, 9
- [39] X. L. Li, J. Thickstun, I. Gulrajani, P. Liang, and T. B. Hashimoto, "Diffusion-lm improves controllable text generation," *arXiv preprint arXiv:2205.14217*, 2022. (document), 4.2.1, 3, 9
- [40] T. Chen, R. Zhang, and G. Hinton, "Analog bits: Generating discrete data using diffusion models with self-conditioning," *arXiv preprint arXiv:2208.04202*, 2022. (document), 4.2.1, 3, 9
- [41] Y. Tashiro, J. Song, Y. Song, and S. Ermon, "Csd: Conditional score-based diffusion models for probabilistic time series imputation," *NIPS*, vol. 34, pp. 24804–24816, 2021. (document), 2.4.2, 4.2.2, 3, 9
- [42] J. M. L. Alcaraz and N. Strodthoff, "Diffusion-based time series imputation and forecasting with structured state space models," *arXiv preprint arXiv:2208.09399*, 2022. (document), 4.2.2, 3, 9
- [43] N. Chen, Y. Zhang, H. Zen, R. J. Weiss, M. Norouzi, and W. Chan, "Wavegrad: Estimating gradients for waveform generation," in *ICLR*, 2020. (document), 4.3, 3, 9
- [44] Z. Kong, W. Ping, J. Huang, K. Zhao, and B. Catanzaro, "Diffwave: A versatile diffusion model for audio synthesis," in *ICLR*, 2020. (document), 4.3, 3, 9
- [45] V. Popov, I. Vovk, V. Gogoryan, T. Sadekova, and M. Kudinov, "Grad-tts: A diffusion probabilistic model for text-to-speech," in *ICML*. PMLR, 2021, pp. 8599–8608. (document), 4.3, 9
- [46] J. Liu, C. Li, Y. Ren, F. Chen, and Z. Zhao, "Diffinger: Singing voice synthesis via shallow diffusion mechanism," in *AAAI*, vol. 36, no. 10, 2022, pp. 11 020–11 028. (document), 4.3, 3, 9
- [47] J. Tae, H. Kim, and T. Kim, "Editts: Score-based editing for controllable text-to-speech," *arXiv preprint arXiv:2110.02584*, 2021. (document), 4.3, 3, 9
- [48] H. Kim, S. Kim, and S. Yoon, "Guided-tts: A diffusion model for text-to-speech via classifier guidance," in *ICML*. PMLR, 2022, pp. 11 119–11 133. (document), 3.2, 4.3, 3, 9
- [49] S. Kim, H. Kim, and S. Yoon, "Guided-tts 2: A diffusion model for high-quality adaptive text-to-speech with untranscribed data," *arXiv preprint arXiv:2205.15370*, 2022. (document), 4.3, 3, 9
- [50] Y. Koizumi, H. Zen, K. Yatabe, N. Chen, and M. Bacchiani, "Specgrad: Diffusion probabilistic model based neural vocoder with adaptive noise spectral shaping," *arXiv preprint arXiv:2203.16749*, 2022. (document), 4.3, 3, 9
- [51] Z. Kong, W. Ping, J. Huang, K. Zhao, and B. Catanzaro, "Diffwave: A versatile diffusion model for audio synthesis," 2020. [Online]. Available: <https://arxiv.org/abs/2009.09761> (document)
- [52] H. Kim, S. Kim, and S. Yoon, "Guided-tts: A diffusion model for text-to-speech via classifier guidance," 2021. [Online]. Available: <https://arxiv.org/abs/2111.11755> (document)
- [53] S. Luo, C. Shi, M. Xu, and J. Tang, "Predicting molecular conformation via dynamic graph score matching," *NIPS*, vol. 34, pp. 19784–19795, 2021. (document), 4.4.1, 3, 9
- [54] M. Xu, L. Yu, Y. Song, C. Shi, S. Ermon, and J. Tang, "Geodiff: A geometric diffusion model for molecular conformation generation," in *ICLR*, 2021. (document), 4.4.1, 3, 9
- [55] B. Jing, G. Corso, R. Barzilay, and T. S. Jaakkola, "Torsional diffusion for molecular conformer generation," in *ICLR*, 2022. (document), 3.2, 4.4.1, 3, 9
- [56] S. Luo, Y. Su, X. Peng, S. Wang, J. Peng, and J. Ma, "Antigen-specific antibody design and optimization with diffusion-based generative models," *bioRxiv*, 2022. (document), 4.4.2, 3, 9
- [57] N. Anand and T. Achim, "Protein structure and sequence generation with equivariant denoising diffusion probabilistic models," *arXiv preprint arXiv:2205.15019*, 2022. (document), 3.2.3, 3, 4.4.2, 9
- [58] I. J. Goodfellow, J. Pouget-Abadie, M. Mirza, B. Xu, D. Warde-Farley, S. Ozair, A. Courville, and Y. Bengio, "Generative adversarial networks," 2014. [Online]. Available: <https://arxiv.org/abs/1406.2661>
- [59] I. Goodfellow, Y. Bengio, and A. Courville, *Deep Learning*. MIT Press, 2016, <http://www.deeplearningbook.org>. 1
- [60] D. P. Kingma and M. Welling, "Auto-encoding variational bayes," *arXiv preprint arXiv:1312.6114*, 2013. 1
- [61] A. Q. Nichol and P. Dhariwal, "Improved denoising diffusion probabilistic models," in *ICML*. PMLR, 2021, pp. 8162–8171. (document), 2.3.1, 3.1.1, 2, 3.3, 3.3.1, B.3, 6, 7, 8
- [62] T. Salimans and J. Ho, "Progressive distillation for fast sampling of diffusion models," *arXiv preprint arXiv:2202.00512*, 2022. (document), 3, 3.1.1, 2, 7, 8
- [63] Z. Xiao, K. Kreis, and A. Vahdat, "Tackling the generative learning trilemma with denoising diffusion gans," *arXiv preprint arXiv:2112.07804*, 2021. (document), 2, 3.1.3, 7, 8
- [64] C. Lu, Y. Zhou, F. Bao, J. Chen, C. Li, and J. Zhu, "Dpm-solver: A fast ode solver for diffusion probabilistic model sampling in around 10 steps," *arXiv preprint arXiv:2206.00927*, 2022. (document), 2.2.3, 2, 3.1.2, 3.1.2, 4, 5, 7, 8
- [65] J. Austin, D. D. Johnson, J. Ho, D. Tarlow, and R. van den Berg, "Structured denoising diffusion models in discrete state-spaces," *NIPS*, vol. 34, pp. 17981–17993, 2021. (document), 2, 3.2.2, 3.3.1, 3, 6, 8, 9
- [66] Y. Song, J. Sohl-Dickstein, D. P. Kingma, A. Kumar, S. Ermon, and B. Poole, "Score-based generative modeling through stochastic differential equations," *arXiv preprint arXiv:2011.13456*, 2020. 2.1.3, 2.2.3, 2.2.3, 2.2.3, 2, 3.1.2, 3.1.4, 3.2.3, 3, 3, 6, 8

- [67] D. Kingma, T. Salimans, B. Poole, and J. Ho, "Variational diffusion models," *NIPS*, vol. 34, pp. 21 696–21 707, 2021. 2.1.3, 3.1.1, 2, 3.1.4, 3.3.1, 6, 8
- [68] J. Ho, A. Jain, and P. Abbeel, "Denosing diffusion probabilistic models," *NIPS*, 2020. 2.2.1, 2.2.1, 2.2.1, 3.3, 3, 1, 6, 8
- [69] Y. Song and S. Ermon, "Generative modeling by estimating gradients of the data distribution," *NIPS*, vol. 32, 2019. 2.2.2, 2.3.2, 4.1.1, 2, 4, 6, 8
- [70] S. Lyu, "Interpretation and generalization of score matching," *arXiv preprint arXiv:1205.2629*, 2012. 2.2.2
- [71] L. Arnold, "Stochastic differential equations," *New York*, 1974. 2.2.3
- [72] B. Oksendal, *Stochastic differential equations: an introduction with applications*. Springer Science & Business Media, 2013. 2.2.3
- [73] A. Hyvärinen and P. Dayan, "Estimation of non-normalized statistical models by score matching," *Journal of Machine Learning Research*, vol. 6, no. 4, 2005. 2.2.3, 2.3.2
- [74] D. Maoutas, S. Reich, and M. Opper, "Interacting particle solutions of fokker-planck equations through gradient-log-density estimation," *Entropy*, vol. 22, no. 8, p. 802, 2020. 2.2.3
- [75] R. T. Chen, Y. Rubanova, J. Bettencourt, and D. K. Duvenaud, "Neural ordinary differential equations," *NIPS*, vol. 31, 2018. 2.2.3, 3.1.2, 3.1.4
- [76] L. Liu, Y. Ren, Z. Lin, and Z. Zhao, "Pseudo numerical methods for diffusion models on manifolds," *arXiv preprint arXiv:2202.09778*, 2022. 2.2.3, 2, 3.1.2, 3.2.3, 4, 8
- [77] J. Song, C. Meng, and S. Ermon, "Denosing diffusion implicit models," in *ICLR*, 2020. 2.3.1, 2, 3.1.2, 7, 8
- [78] Y. Song, S. Garg, J. Shi, and S. Ermon, "Sliced score matching: A scalable approach to density and score estimation," in *Uncertainty in Artificial Intelligence*. PMLR, 2020, pp. 574–584. 2.3.2, 6
- [79] R. M. Neal, "Annealed importance sampling," *Statistics and computing*, 2001. 2.4.1
- [80] R. W. Hamming, "Stable predictor-corrector methods for ordinary differential equations," *JACM*, vol. 6, no. 1, pp. 37–47, 1959. 2.4.1
- [81] J. R. Dormand and P. J. Prince, "A family of embedded runge-kutta formulae," *Journal of computational and applied mathematics*, vol. 6, no. 1, pp. 19–26, 1980. 2.4.1
- [82] T. Sauer, *Numerical analysis*. Addison-Wesley Publishing Company, 2011. 2.4.1
- [83] W. H. Press, S. A. Teukolsky, W. T. Vetterling, and B. P. Flannery, *Numerical recipes 3rd edition: The art of scientific computing*. Cambridge university press, 2007. 2.4.1
- [84] P. Dhariwal and A. Nichol, "Diffusion models beat gans on image synthesis," *NIPS*, vol. 34, pp. 8780–8794, 2021. 2.4.2, 3, 4
- [85] A. Nichol, P. Dhariwal, A. Ramesh, P. Shyam, P. Mishkin, B. McGrew, I. Sutskever, and M. Chen, "Glide: Towards photorealistic image generation and editing with text-guided diffusion models," *arXiv preprint arXiv:2112.10741*, 2021. 2.4.2, 3.2.2, 4.1.2, 3, 9
- [86] C. Lu, Y. Zhou, F. Bao, J. Chen, C. Li, and J. Zhu, "Dpm-solver++: Fast solver for guided sampling of diffusion probabilistic models," *arXiv preprint arXiv:2211.01095*, 2022. 2.4.2
- [87] C. Meng, R. Gao, D. P. Kingma, S. Ermon, J. Ho, and T. Salimans, "On distillation of guided diffusion models," *arXiv preprint arXiv:2210.03142*, 2022. 2.4.2
- [88] M. Hu, Y. Wang, T.-J. Cham, J. Yang, and P. N. Suganthan, "Global context with discrete diffusion in vector quantised modelling for image generation," in *Proceedings of the IEEE/CVF Conference on Computer Vision and Pattern Recognition*, 2022, pp. 11 502–11 511. 2.4.2
- [89] J. Wolleb, F. Bieder, R. Sandkühler, and P. C. Cattin, "Diffusion models for medical anomaly detection," *arXiv preprint arXiv:2203.04306*, 2022. 2.4.2, 3
- [90] K. Packhäuser, L. Folle, F. Thamm, and A. Maier, "Generation of anonymous chest radiographs using latent diffusion models for training thoracic abnormality classification systems," *arXiv preprint arXiv:2211.01323*, 2022. 2.4.2
- [91] S. Chen, P. Sun, Y. Song, and P. Luo, "Diffusiondet: Diffusion model for object detection," *arXiv preprint arXiv:2211.09788*, 2022. 2.4.2, 3
- [92] D. Baranchuk, I. Rubachev, A. Voynov, V. Khruikov, and A. Babenko, "Label-efficient semantic segmentation with diffusion models," *arXiv preprint arXiv:2112.03126*, 2021. 2.4.2, 3
- [93] V. T. Hu, D. W. Zhang, Y. M. Asano, G. J. Burghouts, and C. G. Snoek, "Self-guided diffusion models," *arXiv preprint arXiv:2210.06462*, 2022. 2.4.2, 6
- [94] C.-H. Chao, W.-F. Sun, B.-W. Cheng, and C.-Y. Lee, "Quasi-conservative score-based generative models," *arXiv preprint arXiv:2209.12753*, 2022. 2.4.2
- [95] H. Chung, B. Sim, and J. C. Ye, "Come-closer-diffuse-faster: Accelerating conditional diffusion models for inverse problems through stochastic contraction," in *CVPR*, 2022. 2.4.2, 3.1.1, 2, 3, 8
- [96] J. Choi, S. Kim, Y. Jeong, Y. Gwon, and S. Yoon, "Ilvr: Conditioning method for denosing diffusion probabilistic models," in *CVPR*, 2021, pp. 14 367–14 376. 2.4.2, 3
- [97] C. Saharia, W. Chan, H. Chang, C. Lee, J. Ho, T. Salimans, D. Fleet, and M. Norouzi, "Palette: Image-to-image diffusion models," in *ACM SIGGRAPH*, 2022, pp. 1–10. 3, 4.1.1, 3, 9
- [98] E. Luhman and T. Luhman, "Knowledge distillation in iterative generative models for improved sampling speed," *arXiv preprint arXiv:2101.02388*, 2021. 3.1.1, 2, 7, 8
- [99] H. Zheng, P. He, W. Chen, and M. Zhou, "Truncated diffusion probabilistic models," *arXiv preprint arXiv:2202.09671*, 2022. 3.1.1, 2, 6, 7, 8
- [100] E. Hoogeboom and T. Salimans, "Blurring diffusion models," *arXiv preprint arXiv:2209.05557*, 2022. 3.1.1, 2
- [101] Z. Lyu, X. Xu, C. Yang, D. Lin, and B. Dai, "Accelerating diffusion models via early stop of the diffusion process," *arXiv preprint arXiv:2205.12524*, 2022. 3.1.1, 2, 3.1.3, 4, 5, 7, 8
- [102] G. Daras, M. Delbracio, H. Talebi, A. G. Dimakis, and P. Milanfar, "Soft diffusion: Score matching for general corruptions," *arXiv preprint arXiv:2209.05442*, 2022. 3.1.1, 2
- [103] G. Franzese, S. Rossi, L. Yang, A. Finamore, D. Rossi, M. Filippone, and P. Michiardi, "How much is enough? a study on diffusion times in score-based generative models," 2022. [Online]. Available: <https://arxiv.org/abs/2206.05173> 3.1.1, 2, 7, 8
- [104] V. Khruikov and I. Oseledets, "Understanding ddpm latent codes through optimal transport," *arXiv preprint arXiv:2202.07477*, 2022. 2
- [105] Z. Kong and W. Ping, "On fast sampling of diffusion probabilistic models," *arXiv preprint arXiv:2106.00132*, 2021. 3.1.1, 2, 3.1.2, 3.1.4, 7, 8
- [106] R. San-Roman, E. Nachmani, and L. Wolf, "Noise estimation for generative diffusion models," *arXiv preprint arXiv:2104.02600*, 2021. 2, 8
- [107] F. Bao, C. Li, J. Zhu, and B. Zhang, "Analytic-dpm: an analytic estimate of the optimal reverse variance in diffusion probabilistic models," *arXiv preprint arXiv:2201.06503*, 2022. 2, 3.1.2, 3.3.1, 4, 5, 6, 7, 8
- [108] F. Bao, C. Li, J. Sun, J. Zhu, and B. Zhang, "Estimating the optimal covariance with imperfect mean in diffusion probabilistic models," *arXiv preprint arXiv:2206.07309*, 2022. 2, 3.1.2, 4, 5, 6, 7, 8
- [109] Q. Zhang and Y. Chen, "Fast sampling of diffusion models with exponential integrator," *arXiv preprint arXiv:2204.13902*, 2022. 2, 3.1.2, 6, 7, 8
- [110] Q. Zhang, M. Tao, and Y. Chen, "gddim: Generalized denosing diffusion implicit models," *arXiv preprint arXiv:2206.05564*, 2022. 2, 3.1.2, 3.1.4, 7, 8
- [111] D. Watson, J. Ho, M. Norouzi, and W. Chan, "Learning to efficiently sample from diffusion probabilistic models," *arXiv preprint arXiv:2106.03802*, 2021. 2, 3.1.2, 3.1.4, 5, 8
- [112] T. Karras, M. Aittala, T. Aila, and S. Laine, "Elucidating the design space of diffusion-based generative models," *arXiv preprint arXiv:2206.00364*, 2022. 2, 3.1.2, 7, 8
- [113] A. Jolicœur-Martineau, K. Li, R. Piché-Taillefer, T. Kachman, and I. Mitliagkas, "Gotta go fast when generating data with score-based models," *arXiv preprint arXiv:2105.14080*, 2021. 2, 3.1.2, 6, 7
- [114] B. Kim and J. C. Ye, "Denosing mcmc for accelerating diffusion-based generative models," *arXiv preprint arXiv:2209.14593*, 2022. 2, 3.1.2
- [115] D. Watson, W. Chan, J. Ho, and M. Norouzi, "Learning fast samplers for diffusion models by differentiating through sample quality." 2, 5, 7, 8
- [116] K. Pandey, A. Mukherjee, P. Rai, and A. Kumar, "Diffusevae: Efficient, controllable and high-fidelity generation from low-

- dimensional latents," 2022. [Online]. Available: <https://arxiv.org/abs/2201.00308> 2, 3.1.3, 4, 6, 7, 8
- [117] Q. Zhang and Y. Chen, "Diffusion normalizing flow," *NIPS*, vol. 34, pp. 16280–16291, 2021. 2, 3.1.3, 7, 8
- [118] A. Vahdat, K. Kreis, and J. Kautz, "Score-based generative modeling in latent space," *NIPS*, vol. 34, pp. 11287–11302, 2021. 2, 3.1.3, 3.4, 4.1.2, 7, 8, 9
- [119] Y. Song, C. Durkan, I. Murray, and S. Ermon, "Maximum likelihood training of score-based diffusion models," *NIPS*, vol. 34, pp. 1415–1428, 2021. 2, 3.1.3, 3.2.1, 3.3, 3.3.1, 8
- [120] D. Kim, B. Na, S. J. Kwon, D. Lee, W. Kang, and I.-c. Moon, "Maximum likelihood training of parametrized diffusion model," 2021. 2, 3.1.3, 3.3.2, 3.4, 8
- [121] D. Kim, B. Na, S. J. Kwon, D. Lee, W. Kang, and I.-C. Moon, "Maximum likelihood training of implicit nonlinear diffusion models," *arXiv preprint arXiv:2205.13699*, 2022. 2, 3.4, 6, 8
- [122] R. Gao, Y. Song, B. Poole, Y. N. Wu, and D. P. Kingma, "Learning energy-based models by diffusion recovery likelihood," *arXiv preprint arXiv:2012.08125*, 2020. 2, 3.1.3, 8
- [123] Y. Song and D. P. Kingma, "How to train your energy-based models," *arXiv preprint arXiv:2101.03288*, 2021. 2, 8
- [124] J. Gu, S. Zhai, Y. Zhang, M. A. Bautista, and J. Susskind, "f-dm: A multi-stage diffusion model via progressive signal transformation," *arXiv preprint arXiv:2210.04955*, 2022. 2, 3.1.4
- [125] A. Bansal, E. Borgnia, H.-M. Chu, J. S. Li, H. Kazemi, F. Huang, M. Goldblum, J. Geiping, and T. Goldstein, "Cold diffusion: Inverting arbitrary image transforms without noise," *arXiv preprint arXiv:2208.09392*, 2022. 2, 3.1.4, 3.2.1
- [126] J. Benton, Y. Shi, V. De Bortoli, G. Deligiannidis, and A. Doucet, "From denoising diffusions to denoising markov models," *arXiv preprint arXiv:2211.03595*, 2022. 2, 3.1.4
- [127] W. Gong and Y. Li, "Interpreting diffusion score matching using normalizing flow," *arXiv preprint arXiv:2107.10072*, 2021. 2, 3.1.4
- [128] V. De Bortoli, A. Doucet, J. Heng, and J. Thornton, "Simulating diffusion bridges with score matching," *arXiv preprint arXiv:2111.07243*, 2021. 2, 3.1.4, 8
- [129] C.-W. Huang, J. H. Lim, and A. C. Courville, "A variational perspective on diffusion-based generative models and score matching," *NIPS*, 2021. 2, 3.1.4, 3.3.1, 8
- [130] H. Chung, J. Kim, M. T. Mccann, M. L. Klasky, and J. C. Ye, "Diffusion posterior sampling for general noisy inverse problems," *arXiv preprint arXiv:2209.14687*, 2022. 2, 3.2.1
- [131] B. Kawar, J. Song, S. Ermon, and M. Elad, "Jpeg artifact correction using denoising diffusion restoration models," *arXiv preprint arXiv:2209.11888*, 2022. 2, 3.2.1, 3
- [132] L. Zhou, Y. Du, and J. Wu, "3d shape generation and completion through point-voxel diffusion," in *ICCV*, 2021. 2, 3.2.1, 8
- [133] A.-C. Cheng, X. Li, S. Liu, M. Sun, and M.-H. Yang, "Autoregressive 3d shape generation via canonical mapping," *arXiv preprint arXiv:2204.01955*, 2022. 2, 3.2.1, 3, 9
- [134] E. Hoogeboom, D. Nielsen, P. Jaini, P. Forré, and M. Welling, "Argmax flows and multinomial diffusion: Towards non-autoregressive language models," 2021. 2, 3.2.2, 3, 8, 9
- [135] E. Hoogeboom, A. A. Gritsenko, J. Bastings, B. Poole, R. v. d. Berg, and T. Salimans, "Autoregressive diffusion models," *arXiv preprint arXiv:2110.02037*, 2021. 2, 3.2.2, 8
- [136] A. Campbell, J. Benton, V. De Bortoli, T. Rainforth, G. Deligiannidis, and A. Doucet, "A continuous time framework for discrete denoising models," *arXiv preprint arXiv:2205.14987*, 2022. 2, 8
- [137] S. Gu, D. Chen, J. Bao, F. Wen, B. Zhang, D. Chen, L. Yuan, and B. Guo, "Vector quantized diffusion model for text-to-image synthesis," in *CVPR*, 2022, pp. 10696–10706. 2, 3.2.2, 8, 9
- [138] Z. Tang, S. Gu, J. Bao, D. Chen, and F. Wen, "Improved vector quantized diffusion models," *arXiv preprint arXiv:2205.16007*, 2022. 2, 3.2.2, 3, 8, 9
- [139] M. Cohen, G. Quispe, S. L. Corff, C. Ollion, and E. Moulines, "Diffusion bridges vector quantized variational autoencoders," *arXiv preprint arXiv:2202.04895*, 2022. 2, 3.2.2, 8
- [140] P. Xie, Q. Zhang, Z. Li, H. Tang, Y. Du, and X. Hu, "Vector quantized diffusion model with codeunet for text-to-sign pose sequences generation," *arXiv preprint arXiv:2208.09141*, 2022. 2, 3.2.2, 8, 9
- [141] C. Guo, S. Zou, X. Zuo, S. Wang, W. Ji, X. Li, and L. Cheng, "Generating diverse and natural 3d human motions from text," in *Proceedings of the IEEE/CVF Conference on Computer Vision and Pattern Recognition*, 2022, pp. 5152–5161. 2, 3.2.2, 3.2.3
- [142] S. Weinbach, M. Bellagente, C. Eichenberg, A. Dai, R. Baldock, S. Nanda, B. Deiseroth, K. Oostermeijer, H. Teufel, and A. F. Cruz-Salinas, "M-vader: A model for diffusion with multimodal context," *arXiv preprint arXiv:2212.02936*, 2022. 2, 3.2.2
- [143] X. Xu, Z. Wang, E. Zhang, K. Wang, and H. Shi, "Versatile diffusion: Text, images and variations all in one diffusion model," *arXiv preprint arXiv:2211.08332*, 2022. 2, 3.2.2
- [144] V. De Bortoli, E. Mathieu, M. Hutchinson, J. Thornton, Y. W. Teh, and A. Doucet, "Riemannian score-based generative modeling," *arXiv preprint arXiv:2202.02763*, 2022. 2, 3.2.3, 8
- [145] C.-W. Huang, M. Aghajohari, A. J. Bose, P. Panangaden, and A. Courville, "Riemannian diffusion models," *arXiv preprint arXiv:2208.07949*, 2022. 2, 3.2.3, 8
- [146] L. Luzi, A. Siahkoobi, P. M. Mayer, J. Casco-Rodriguez, and R. Baraniuk, "Boomerang: Local sampling on image manifolds using diffusion models," *arXiv preprint arXiv:2210.12100*, 2022. 2, 3.2.3
- [147] X. Cheng, J. Zhang, and S. Sra, "Theory and algorithms for diffusion processes on riemannian manifolds," *arXiv preprint arXiv:2204.13665*, 2022. 2, 3.2.3
- [148] C. Niu, Y. Song, J. Song, S. Zhao, A. Grover, and S. Ermon, "Permutation invariant graph generation via score-based generative modeling," in *AISTATS*. PMLR, 2020, pp. 4474–4484. 2, 3.2.3, 8
- [149] H. Huang, L. Sun, B. Du, Y. Fu, and W. Lv, "Graphgdp: Generative diffusion processes for permutation invariant graph generation," *arXiv preprint arXiv:2212.01842*, 2022. 2, 3.2.3
- [150] X. Chen, Y. Li, A. Zhang, and L.-p. Liu, "Nvdif: Graph generation through the diffusion of node vectors," *arXiv preprint arXiv:2211.10794*, 2022. 2, 3.2.3
- [151] T. Luo, Z. Mo, and S. J. Pan, "Fast graph generative model via spectral diffusion," *arXiv preprint arXiv:2211.08892*, 2022. 2, 3.2.3
- [152] D. Kim, S. Shin, K. Song, W. Kang, and I.-C. Moon, "Soft truncation: A universal training technique of score-based diffusion model for high precision score estimation," 2021. [Online]. Available: <https://arxiv.org/abs/2106.05527> 2, 3.3.1, 3.3.1, 4, 6, 8
- [153] H. Zhang, R. Feng, Z. Yang, L. Huang, Y. Liu, Y. Zhang, Y. Shen, D. Zhao, J. Zhou, and F. Cheng, "Dimensionality-varying diffusion process," *arXiv preprint arXiv:2211.16032*, 2022. 2, 3.4
- [154] R. G. Lopes, S. Fenu, and T. Starmer, "Data-free knowledge distillation for deep neural networks," *arXiv preprint arXiv:1710.07535*, 2017. 3.1.1
- [155] J. Gou, B. Yu, S. J. Maybank, and D. Tao, "Knowledge distillation: A survey," *IJCV*, vol. 129, no. 6, pp. 1789–1819, 2021. 3.1.1
- [156] T. Choudhary, V. Mishra, A. Goswami, and J. Sarangapani, "A comprehensive survey on model compression and acceleration," *Artificial Intelligence Review*, 2020. 3.1.1
- [157] Y. Cheng, D. Wang, P. Zhou, and T. Zhang, "A survey of model compression and acceleration for deep neural networks," *arXiv preprint arXiv:1710.09282*, 2017. 3.1.1
- [158] H. Tsukamoto, S.-J. Chung, and J.-J. E. Slotine, "Contraction theory for nonlinear stability analysis and learning-based control: A tutorial overview," *Annual Reviews in Control*, 2021. 3.1.1
- [159] N. V. Hung, S. Migórski, V. M. Tam, and S. Zeng, "Gap functions and error bounds for variational-hemivariational inequalities," *Acta Applicandae Mathematicae*, 2020. 3.1.1
- [160] H. Zheng and M. Zhou, "Act: Asymptotic conditional transport," 2020. 3.1.1
- [161] Q. Han and S. Ji, "Novel multi-step predictor-corrector schemes for backward stochastic differential equations," *arXiv preprint arXiv:2102.05915*, 2021. 3.1.2, 3.1.2
- [162] E. Süli and D. F. Mayers, *An introduction to numerical analysis*. Cambridge university press, 2003. 3.1.2
- [163] C. W. Gear and D. R. Wells, "Multirate linear multistep methods," *BIT Numerical Mathematics*, vol. 24, no. 4, pp. 484–502, 1984. 3.1.2
- [164] L. F. Shampine, *Numerical solution of ordinary differential equations*. Routledge, 2018. 3.1.2
- [165] M. Hochbruck and A. Ostermann, "Exponential integrators," *Acta Numerica*, vol. 19, pp. 209–286, 2010. 3.1.2
- [166] R. Bellman, "Dynamic programming," *Science*, 1966. 3.1.2
- [167] R. E. Bellman and S. E. Dreyfus, *Applied dynamic programming*, 2015. 3.1.2
- [168] D. Watson, W. Chan, J. Ho, and M. Norouzi, "Learning fast samplers for diffusion models by differentiating through sample quality," in *ICLR*, 2021. 3.1.2
- [169] R. Gao, X. Hou, J. Qin, J. Chen, L. Liu, F. Zhu, Z. Zhang, and L. Shao, "Zero-vae-gan: Generating unseen features for general-

- ized and transductive zero-shot learning," *IEEE Transactions on Image Processing*, 2020. 3.1.3
- [170] Z. Niu, K. Yu, and X. Wu, "Lstm-based vae-gan for time-series anomaly detection," *Sensors*, 2020. 3.1.3
- [171] A. Grover, M. Dhar, and S. Ermon, "Flow-gan: Combining maximum likelihood and adversarial learning in generative models," in *AAAI*, 2018. 3.1.3
- [172] Z. Xiao, Q. Yan, and Y. Amit, "Generative latent flow," *arXiv preprint arXiv:1905.10485*, 2019. 3.1.3
- [173] E. Hoogeboom, T. S. Cohen, and J. M. Tomczak, "Learning discrete distributions by dequantization," *arXiv preprint arXiv:2001.11235*, 2020. 3.1.3
- [174] K. Lee, W. Xu, F. Fan, and Z. Tu, "Wasserstein introspective neural networks," in *CVPR*, 2018, pp. 3702–3711. 3.1.3
- [175] W. Grathwohl, R. T. Chen, J. Bettencourt, I. Sutskever, and D. Duvenaud, "Fjord: Free-form continuous dynamics for scalable reversible generative models," *arXiv preprint arXiv:1810.01367*, 2018. 3.1.4
- [176] L. Alili, P. Graczyk, and T. Zak, "On inversions and doob h-transforms of linear diffusions," *Lecture Notes in Mathematics*, 2012. 3.1.4
- [177] V. Dutordoir, A. Saul, Z. Ghahramani, and F. Simpson, "Neural diffusion processes," *arXiv preprint arXiv:2206.03992*, 2022. 3.2.1
- [178] A. Vaswani, N. Shazeer, N. Parmar, J. Uszkoreit, L. Jones, A. N. Gomez, Ł. Kaiser, and I. Polosukhin, "Attention is all you need," *NIPS*, 2017. 3.2.2
- [179] J. Devlin, M.-W. Chang, K. Lee, and K. Toutanova, "Bert: Pre-training of deep bidirectional transformers for language understanding," *arXiv preprint arXiv:1810.04805*, 2018. 3.2.2
- [180] A. Ramesh, P. Dhariwal, A. Nichol, C. Chu, and M. Chen, "Hierarchical text-conditional image generation with clip latents," *arXiv preprint arXiv:2204.06125*, 2022. 3.2.2
- [181] J. Jumper, R. Evans, A. Pritzel, T. Green, M. Figurnov, O. Ronneberger, K. Tunyasuvunakool, R. Bates, A. Židek, A. Potapenko *et al.*, "Highly accurate protein structure prediction with alphafold," *Nature*, 2021. 3.2.2
- [182] S. Ovchinnikov and P.-S. Huang, "Structure-based protein design with deep learning," *Current opinion in chemical biology*, 2021. 3.2.2
- [183] A. Van Den Oord, O. Vinyals *et al.*, "Neural discrete representation learning," *NIPS*, vol. 30, 2017. 3.2.2, 3.3
- [184] W. Fan, Y. Ma, Q. Li, Y. He, E. Zhao, J. Tang, and D. Yin, "Graph neural networks for social recommendation," in *The world wide web conference*, 2019. 3.2.3
- [185] C. Huang, H. Xu, Y. Xu, P. Dai, L. Xia, M. Lu, L. Bo, H. Xing, X. Lai, and Y. Ye, "Knowledge-aware coupled graph neural network for social recommendation," in *AAAI*, 2021. 3.2.3
- [186] B. Jing, S. Eismann, P. Suriana, R. J. L. Townshend, and R. Dror, "Learning from protein structure with geometric vector perceptrons," in *ICLR*, 2020. 3.2.3
- [187] V. G. Satorras, E. Hoogeboom, and M. Welling, "E (n) equivariant graph neural networks," in *ICML*. PMLR, 2021. 3.2.3
- [188] H. Lin, Z. Gao, Y. Xu, L. Wu, L. Li, and S. Z. Li, "Conditional local convolution for spatio-temporal meteorological forecasting," in *AAAI*, 2022. 3.2.3
- [189] B. Yu, H. Yin, and Z. Zhu, "Spatio-temporal graph convolutional networks: A deep learning framework for traffic forecasting," *arXiv preprint arXiv:1709.04875*, 2017. 3.2.3
- [190] H. A. Pierson and M. S. Gashler, "Deep learning in robotics: a review of recent research," *Advanced Robotics*, 2017. 3.2.3
- [191] R. P. De Lima, K. Marfurt, D. Duarte, and A. Bonar, "Progress and challenges in deep learning analysis of geoscience images," in *81st EAGE Conference and Exhibition 2019*. European Association of Geoscientists & Engineers, 2019. 3.2.3
- [192] J. Wang, H. Cao, J. Z. Zhang, and Y. Qi, "Computational protein design with deep learning neural networks," *Scientific reports*, 2018. 3.2.3
- [193] W. Cao, Z. Yan, Z. He, and Z. He, "A comprehensive survey on geometric deep learning," *IEEE Access*, 2020. 3.2.3
- [194] L. Wu, H. Lin, Z. Gao, C. Tan, and S. Z. Li, "Self-supervised on graphs: Contrastive, generative, or predictive," 2021. 3.2.3
- [195] H. Lin, Y. Huang, M. Liu, X. Li, S. Ji, and S. Z. Li, "Diffbp: Generative diffusion of 3d molecules for target protein binding," *arXiv preprint arXiv:2211.11214*, 2022. 3.2.3, 3
- [196] I. Higgins, L. Matthey, A. Pal, C. Burgess, X. Glorot, M. Botvinick, S. Mohamed, and A. Lerchner, "beta-vae: Learning basic visual concepts with a constrained variational framework," 2016. 3.3
- [197] F. Vargas, P. Thodoroff, A. Lamacraft, and N. Lawrence, "Solving schrödinger bridges via maximum likelihood," *Entropy*, 2021. 3.3.1
- [198] V. De Bortoli, J. Thornton, J. Heng, and A. Doucet, "Diffusion schrödinger bridge with applications to score-based generative modeling," *NIPS*, 2021. 3.3.1
- [199] C. Cremer, X. Li, and D. Duvenaud, "Inference suboptimality in variational autoencoders," in *ICML*, 2018. 3.3.2
- [200] A. Ulhaq, N. Akhtar, and G. Pogrebná, "Efficient diffusion models for vision: A survey," *arXiv preprint arXiv:2210.09292*, 2022. 4
- [201] B. Kawar, M. Elad, S. Ermon, and J. Song, "Denoising diffusion restoration models," in *ICLR Workshop*, 2022. 4.1.1, 3, 9
- [202] L. Theis, T. Salimans, M. D. Hoffman, and F. Mentzer, "Lossy compression with gaussian diffusion," *arXiv preprint arXiv:2206.08889*, 2022. 4.1.1, 9
- [203] A. Lugmayr, M. Danelljan, A. Romero, F. Yu, R. Timofte, and L. Van Gool, "Repaint: Inpainting using denoising diffusion probabilistic models," in *CVPR*, 2022, pp. 11461–11471. 4.1.1, 3, 9
- [204] A. Radford, J. W. Kim, C. Hallacy, A. Ramesh, G. Goh, S. Agarwal, G. Sastry, A. Askell, P. Mishkin, J. Clark *et al.*, "Learning transferable visual models from natural language supervision," in *ICML*. PMLR, 2021, pp. 8748–8763. 4.1.2, 6
- [205] B. Poole, A. Jain, J. T. Barron, and B. Mildenhall, "Dreamfusion: Text-to-3d using 2d diffusion," *arXiv preprint arXiv:2209.14988*, 2022. 4.1.2, 3, 9
- [206] T. Amit, E. Nachmani, T. Shaharabany, and L. Wolf, "Segdiff: Image segmentation with diffusion probabilistic models," *arXiv preprint arXiv:2112.00390*, 2021. 4.1.2, 3, 9
- [207] A. Krizhevsky, I. Sutskever, and G. E. Hinton, "Imagenet classification with deep convolutional neural networks," *Communications of the ACM*, vol. 60, no. 6, pp. 84–90, 2017. C
- [208] T.-Y. Lin, M. Maire, S. Belongie, J. Hays, P. Perona, D. Ramanan, P. Dollár, and C. L. Zitnick, "Microsoft coco: Common objects in context," in *ECCV*. Springer, 2014, pp. 740–755. 4.1.2
- [209] P. Sanchez and S. A. Tsafaris, "Diffusion causal models for counterfactual estimation," in *First Conference on Causal Learning and Reasoning*, 2021. 4.1.2
- [210] L. Zhou, Y. Du, and J. Wu, "3d shape generation and completion through point-voxel diffusion," in *ICCV*, 2021, pp. 5826–5835. 4.1.3, 3, 9
- [211] R. Yang, P. Srivastava, and S. Mandt, "Diffusion probabilistic modeling for video generation," *arXiv preprint arXiv:2203.09481*, 2022. 4.1.4, 3, 9
- [212] W. Harvey, S. Naderiparizi, V. Masrani, C. Weibach, and F. Wood, "Flexible diffusion modeling of long videos," *arXiv preprint arXiv:2205.11495*, 2022. 4.1.4, 3, 9
- [213] Y. Song, L. Shen, L. Xing, and S. Ermon, "Solving inverse problems in medical imaging with score-based generative models," in *ICLR*, 2021. 4.1.5, 3, 9
- [214] H. Chung, E. S. Lee, and J. C. Ye, "Mr image denoising and super-resolution using regularized reverse diffusion," *arXiv preprint arXiv:2203.12621*, 2022. 4.1.5, 3, 9
- [215] P. Sanchez, A. Kascenas, X. Liu, A. Q. O'Neil, and S. A. Tsafaris, "What is healthy? generative counterfactual diffusion for lesion localization," *arXiv preprint arXiv:2207.12268*, 2022. 4.1.5
- [216] J. Singh, S. Gould, and L. Zheng, "High-fidelity guided image synthesis with latent diffusion models," *arXiv preprint arXiv:2211.17084*, 2022. 3
- [217] S. Welker, H. N. Chapman, and T. Gerkmann, "Driftrec: Adapting diffusion models to blind image restoration tasks," *arXiv preprint arXiv:2211.06757*, 2022. 3
- [218] Y. Yin, L. Huang, Y. Liu, and K. Huang, "Diffgar: Model-agnostic restoration from generative artifacts using image-to-image diffusion models," *arXiv preprint arXiv:2210.08573*, 2022. 3
- [219] J. Whang, M. Delbracio, H. Talebi, C. Saharia, A. G. Dimakis, and P. Milanfar, "Deblurring via stochastic refinement," in *Proceedings of the IEEE/CVF Conference on Computer Vision and Pattern Recognition*, 2022, pp. 16293–16303. 3
- [220] G. Batzolis, J. Stanczuk, C.-B. Schönlieb, and C. Etmann, "Non-uniform diffusion models," *arXiv preprint arXiv:2207.09786*, 2022. 3
- [221] M. Ren, M. Delbracio, H. Talebi, G. Gerig, and P. Milanfar, "Image deblurring with domain generalizable diffusion models," *arXiv preprint arXiv:2212.01789*, 2022. 3

- [222] X. Wang, J.-K. Yan, J.-Y. Cai, J.-H. Deng, Q. Qin, Q. Wang, H. Xiao, Y. Cheng, and P.-F. Ye, "Superresolution reconstruction of single image for latent features," *arXiv preprint arXiv:2211.12845*, 2022. 3
- [223] V. Voleti, C. Pal, and A. Oberman, "Score-based denoising diffusion with non-isotropic gaussian noise models," *arXiv preprint arXiv:2210.12254*, 2022. 3
- [224] T. Dockhorn, A. Vahdat, and K. Kreis, "Genie: Higher-order denoising diffusion solvers," *arXiv preprint arXiv:2210.05475*, 2022. 3
- [225] Y. Nikankin, N. Haim, and M. Irani, "Sinfusion: Training diffusion models on a single image or video," *arXiv preprint arXiv:2211.11743*, 2022. 3
- [226] G. Kwon and J. C. Ye, "Diffusion-based image translation using disentangled style and content representation," *arXiv preprint arXiv:2209.15264*, 2022. 3
- [227] X. Su, J. Song, C. Meng, and S. Ermon, "Dual diffusion implicit bridges for image-to-image translation," *arXiv preprint arXiv:2203.08382*, 2022. 3
- [228] B. Kolbeinsson and K. Mikolajczyk, "Multi-class segmentation from aerial views using recursive noise diffusion," *arXiv preprint arXiv:2212.00787*, 2022. 3
- [229] Z. Gu, H. Chen, Z. Xu, J. Lan, C. Meng, and W. Wang, "Diffusion-inst: Diffusion model for instance segmentation," *arXiv preprint arXiv:2212.02773*, 2022. 3
- [230] J. Wolleb, R. Sandkühler, F. Bieder, P. Valmaggia, and P. C. Cattin, "Diffusion models for implicit image segmentation ensembles," *arXiv preprint arXiv:2112.03145*, 2021. 3
- [231] C. Saharia, W. Chan, S. Saxena, L. Li, J. Whang, E. Denton, S. K. S. Ghasemipour, B. K. Ayan, S. S. Mahdavi, R. G. Lopes *et al.*, "Photorealistic text-to-image diffusion models with deep language understanding," *arXiv preprint arXiv:2205.11487*, 2022. 3
- [232] G. Kim and J. C. Ye, "Diffusionclip: Text-guided image manipulation using diffusion models," 2021. 3
- [233] G. Li, H. Zheng, C. Wang, C. Li, C. Zheng, and D. Tao, "3ddesigner: Towards photorealistic 3d object generation and editing with text-guided diffusion models," *arXiv preprint arXiv:2211.14108*, 2022. 3
- [234] X. Zeng, A. Vahdat, F. Williams, Z. Gojcic, O. Litany, S. Fidler, and K. Kreis, "Lion: Latent point diffusion models for 3d shape generation," *arXiv preprint arXiv:2210.06978*, 2022. 3
- [235] G. Metzger, E. Richardson, O. Patashnik, R. Giryes, and D. Cohen-Or, "Latent-nerf for shape-guided generation of 3d shapes and textures," *arXiv preprint arXiv:2211.07600*, 2022. 3
- [236] G. Nam, M. Khelifi, A. Rodriguez, A. Tono, L. Zhou, and P. Guerrero, "3d-ldm: Neural implicit 3d shape generation with latent diffusion models," *arXiv preprint arXiv:2212.00842*, 2022. 3
- [237] J. R. Shue, E. R. Chan, R. Po, Z. Ankner, J. Wu, and G. Wetzstein, "3d neural field generation using triplane diffusion," *arXiv preprint arXiv:2211.16677*, 2022. 3
- [238] G. Shim, M. Lee, and J. Choo, "Refu: Refine and fuse the unobserved view for detail-preserving single-image 3d human reconstruction," in *Proceedings of the 30th ACM International Conference on Multimedia*, 2022, pp. 6850–6859. 3
- [239] D. Wei, H. Sun, B. Li, J. Lu, W. Li, X. Sun, and S. Hu, "Human joint kinematics diffusion-refinement for stochastic motion prediction," *arXiv preprint arXiv:2210.05976*, 2022. 3
- [240] Y. Yuan, J. Song, U. Iqbal, A. Vahdat, and J. Kautz, "Physdiff: Physics-guided human motion diffusion model," *arXiv preprint arXiv:2212.02500*, 2022. 3
- [241] J. Gong, L. G. Foo, Z. Fan, Q. Ke, H. Rahmani, and J. Liu, "Diffpose: Toward more reliable 3d pose estimation," *arXiv preprint arXiv:2211.16940*, 2022. 3
- [242] K. Holmquist and B. Wandt, "Diffpose: Multi-hypothesis human pose estimation using diffusion models," *arXiv preprint arXiv:2211.16487*, 2022. 3
- [243] G. Tevet, S. Raab, B. Gordon, Y. Shafir, D. Cohen-Or, and A. H. Bermano, "Human motion diffusion model," *arXiv preprint arXiv:2209.14916*, 2022. 3
- [244] Y.-C. Cheng, H.-Y. Lee, S. Tulyakov, A. Schwing, and L. Gui, "Sdfusion: Multimodal 3d shape completion, reconstruction, and generation," *arXiv preprint arXiv:2212.04493*, 2022. 3
- [245] K. Mei and V. M. Patel, "Vidm: Video implicit diffusion models," *arXiv preprint arXiv:2212.00235*, 2022. 3
- [246] U. Singer, A. Polyak, T. Hayes, X. Yin, J. An, S. Zhang, Q. Hu, H. Yang, O. Ashual, O. Gafni *et al.*, "Make-a-video: Text-to-video generation without text-video data," *arXiv preprint arXiv:2209.14792*, 2022. 3
- [247] G. Kim, H. Shim, H. Kim, Y. Choi, J. Kim, and E. Yang, "Diffusion video autoencoders: Toward temporally consistent face video editing via disentangled video encoding," *arXiv preprint arXiv:2212.02802*, 2022. 3
- [248] Z.-X. Cui, C. Cao, S. Liu, Q. Zhu, J. Cheng, H. Wang, Y. Zhu, and D. Liang, "Self-score: Self-supervised learning on score-based models for mri reconstruction," *arXiv preprint arXiv:2209.00835*, 2022. 3
- [249] A. Jalal, M. Arvinte, G. Daras, E. Price, A. G. Dimakis, and J. Tamir, "Robust compressed sensing mri with deep generative priors," *Advances in Neural Information Processing Systems*, vol. 34, pp. 14 938–14 954, 2021. 3
- [250] P. Rouzrokh, B. Khosravi, S. Faghani, M. Moassefi, S. Vahdati, and B. J. Erickson, "Multitask brain tumor inpainting with diffusion models: A methodological report," *arXiv preprint arXiv:2210.12113*, 2022. 3
- [251] J. Wyatt, A. Leach, S. M. Schmon, and C. G. Willcocks, "Anodpdm: Anomaly detection with denoising diffusion probabilistic models using simplex noise," in *Proceedings of the IEEE/CVF Conference on Computer Vision and Pattern Recognition*, 2022, pp. 650–656. 3
- [252] J. Wu, H. Fang, Y. Zhang, Y. Yang, and Y. Xu, "Medsegdiff: Medical image segmentation with diffusion probabilistic model," *arXiv preprint arXiv:2211.00611*, 2022. 3
- [253] Z. He, T. Sun, K. Wang, X. Huang, and X. Qiu, "Diffusionbert: Improving generative masked language models with diffusion models," *arXiv preprint arXiv:2211.15029*, 2022. 3
- [254] S. W. Park, K. Lee, and J. Kwon, "Neural markov controlled sde: Stochastic optimization for continuous-time data," in *ICLR*, 2021. 4.2.2, 3, 9
- [255] K. Rasul, C. Seward, I. Schuster, and R. Vollgraf, "Autoregressive denoising diffusion models for multivariate probabilistic time series forecasting," in *International Conference on Machine Learning*. PMLR, 2021, pp. 8857–8868. 3
- [256] J. Lee and S. Han, "Nu-wave: A diffusion probabilistic model for neural audio upsampling," *arXiv preprint arXiv:2104.02321*, 2021. 3
- [257] Z. Qiu, M. Fu, Y. Yu, L. Yin, F. Sun, and H. Huang, "Srtnet: Time domain speech enhancement via stochastic refinement," *arXiv preprint arXiv:2210.16805*, 2022. 3
- [258] D.-Y. Wu, W.-Y. Hsiao, F.-R. Yang, O. Friedman, W. Jackson, S. Bruzenak, Y.-W. Liu, and Y.-H. Yang, "Ddsp-based singing vocoders: A new subtractive-based synthesizer and a comprehensive evaluation," *arXiv preprint arXiv:2208.04756*, 2022. 3
- [259] D. Yang, J. Yu, H. Wang, W. Wang, C. Weng, Y. Zou, and D. Yu, "Diffsound: Discrete diffusion model for text-to-sound generation," *arXiv preprint arXiv:2207.09983*, 2022. 4.3, 3, 9
- [260] Y. Leng, Z. Chen, J. Guo, H. Liu, J. Chen, X. Tan, D. Mandic, L. He, X.-Y. Li, T. Qin *et al.*, "Binauralgrad: A two-stage conditional diffusion probabilistic model for binaural audio synthesis," *arXiv preprint arXiv:2205.14807*, 2022. 4.3, 3, 9
- [261] R. Scheibler, Y. Ji, S.-W. Chung, J. Byun, S. Choe, and M.-S. Choi, "Diffusion-based generative speech source separation," *arXiv preprint arXiv:2210.17327*, 2022. 3
- [262] S. Han, H. Ihm, D. Ahn, and W. Lim, "Instrument separation of symbolic music by explicitly guided diffusion model," *arXiv preprint arXiv:2209.02696*, 2022. 3
- [263] S. Liu, Y. Cao, D. Su, and H. Meng, "Diffsvc: A diffusion probabilistic model for singing voice conversion," in *IEEE ASRU*, 2021. 3, 9
- [264] V. Popov, I. Vovk, V. Gogoryan, T. Sadekova, M. S. Kudinov, and J. Wei, "Diffusion-based voice conversion with fast maximum likelihood sampling scheme," in *ICLR*, 2021. 4.3, 3, 9
- [265] M. Jeong, H. Kim, S. J. Cheon, B. J. Choi, and N. S. Kim, "Diff-TTS: A Denoising Diffusion Model for Text-to-Speech," in *Proc. Interspeech 2021*, 2021, pp. 3605–3609. 4.3, 3, 9
- [266] A. Levkovitch, E. Nachmani, and L. Wolf, "Zero-shot voice conditioning for denoising diffusion tts models," *arXiv preprint arXiv:2206.02246*, 2022. 4.3, 3, 9
- [267] Z. Chen, X. Tan, K. Wang, S. Pan, D. Mandic, L. He, and S. Zhao, "Infergrad: Improving diffusion models for vocoder by considering inference in training," in *ICASSP. IEEE*, 2022, pp. 8432–8436. 4.3, 3

- [268] C. Shi, S. Luo, M. Xu, and J. Tang, "Learning gradient fields for molecular conformation generation," in *ICML*. PMLR, 2021, pp. 9558–9568. 4.4.1, 3, 9
- [269] T. Xie, X. Fu, O.-E. Ganea, R. Barzilay, and T. S. Jaakkola, "Crystal diffusion variational autoencoder for periodic material generation," in *ICLR*, 2021. 4.4.2, 3, 9
- [270] J. S. Lee and P. M. Kim, "Proteinsgm: Score-based generative modeling for de novo protein design," *bioRxiv*, 2022. 3, 4.4.2, 9
- [271] G. Corso, H. Stärk, B. Jing, R. Barzilay, and T. Jaakkola, "Diffdock: Diffusion steps, twists, and turns for molecular docking," *arXiv preprint arXiv:2210.01776*, 2022. 4.4.1, 3, 9
- [272] A. Schneuing, Y. Du, C. Harris, A. Jamasb, I. Igashov, W. Du, T. Blundell, P. Lió, C. Gomes, M. Welling *et al.*, "Structure-based drug design with equivariant diffusion models," *arXiv preprint arXiv:2210.13695*, 2022. 3
- [273] C. Shi, C. Wang, J. Lu, B. Zhong, and J. Tang, "Protein sequence and structure co-design with equivariant translation," *arXiv preprint arXiv:2210.08761*, 2022. 3
- [274] I. Igashov, H. Stärk, C. Vignac, V. G. Satorras, P. Frossard, M. Welling, M. Bronstein, and B. Correia, "Equivariant 3d-conditional diffusion models for molecular linker design," *arXiv preprint arXiv:2210.05274*, 2022. 3
- [275] K. E. Wu, K. K. Yang, R. v. d. Berg, J. Y. Zou, A. X. Lu, and A. P. Amini, "Protein structure generation via folding diffusion," *arXiv preprint arXiv:2209.15611*, 2022. 3, 4.4.2, 9
- [276] B. L. Trippe, J. Yim, D. Tischer, T. Broderick, D. Baker, R. Barzilay, and T. Jaakkola, "Diffusion probabilistic modeling of protein backbones in 3d for the motif-scaffolding problem," *arXiv preprint arXiv:2206.04119*, 2022. 3
- [277] W. Jin, J. Wohlwend, R. Barzilay, and T. S. Jaakkola, "Iterative refinement graph neural network for antibody sequence-structure co-design," in *ICLR*, 2021. 4.4.2
- [278] T. Fu and J. Sun, "Antibody complementarity determining regions (cdrs) design using constrained energy model," in *SIGKDD*, 2022, pp. 389–399. 4.4.2
- [279] W. Jin, R. Barzilay, and T. Jaakkola, "Antibody-antigen docking and design via hierarchical structure refinement," in *ICML*. PMLR, 2022, pp. 10 217–10 227. 4.4.2
- [280] J. Ho and T. Salimans, "Classifier-free diffusion guidance," *arXiv preprint arXiv:2207.12598*, 2022. 5
- [281] A. Borji, "Pros and cons of gan evaluation measures: New developments," *Computer Vision and Image Understanding*, vol. 215, p. 103329, 2022. B.1
- [282] T. Salimans, I. Goodfellow, W. Zaremba, V. Cheung, A. Radford, and X. Chen, "Improved techniques for training gans," *NIPS*, vol. 29, 2016. B.1
- [283] S. Kullback, *Information theory and statistics*. Courier Corporation, 1997. B.1
- [284] M. Heusel, H. Ramsauer, T. Unterthiner, B. Nessler, and S. Hochreiter, "Gans trained by a two time-scale update rule converge to a local nash equilibrium," in *NIPS*. Curran Associates, Inc. B.2
- [285] A. Razavi, A. Van den Oord, and O. Vinyals, "Generating diverse high-fidelity images with vq-vae-2," *NIPS*, vol. 32, 2019. B.3
- [286] T. M. Nguyen, A. Garg, R. G. Baraniuk, and A. Anandkumar, "Infocnf: Efficient conditional continuous normalizing flow using adaptive solvers," 2019. B.3
- [287] Z. Ziegler and A. Rush, "Latent normalizing flows for discrete sequences," in *ICML*. PMLR, 2019, pp. 7673–7682. B.3
- [288] J. Tomczak and M. Welling, "Vae with a vampprior," in *AISTATS*. PMLR, 2018, pp. 1214–1223. B.3
- [289] O. Rybkin, K. Daniilidis, and S. Levine, "Simple and effective vae training with calibrated decoders," in *ICML*. PMLR, 2021, pp. 9179–9189. B.3
- [290] A. Krizhevsky, G. Hinton *et al.*, "Learning multiple layers of features from tiny images," 2009. C
- [291] Z. Liu, P. Luo, X. Wang, and X. Tang, "Deep learning face attributes in the wild," in *ICCV*, December 2015. C
- [292] F. Yu, A. Seff, Y. Zhang, S. Song, T. Funkhouser, and J. Xiao, "Lsun: Construction of a large-scale image dataset using deep learning with humans in the loop," *arXiv preprint arXiv:1506.03365*, 2015. C
- [293] T. Karras, S. Laine, and T. Aila, "A style-based generator architecture for generative adversarial networks," in *CVPR*, June 2019. C
- [294] Y. LeCun and C. Cortes, "MNIST handwritten digit database." C
- [295] H. Chung, B. Sim, D. Ryu, and J. C. Ye, "Improving diffusion models for inverse problems using manifold constraints," *arXiv preprint arXiv:2206.00941*, 2022. 5
- [296] Y. Song and S. Ermon, "Improved techniques for training score-based generative models," *NIPS*, vol. 33, pp. 12 438–12 448, 2020. 6, 8

APPENDIX A

SAMPLING ALGORITHMS

In this section, we provide a brief guide on current mainstream sampling methods. We divide them into two parts: unconditional sampling and conditional sampling. For unconditional sampling, we present the original sampling algorithms for three landmarks. For conditional sampling, we divide them into the labeled condition and the unlabeled condition.

A.1 Unconditional Sampling

A.1.1 Ancestral Sampling

Algorithm 1 Ancestral Sampling [68]

```

 $x_T \sim \mathcal{N}(0, I)$ 
for  $t = T, \dots, 1$  do
   $z \sim \mathcal{N}(0, I)$ 
   $x_{t-1} = \frac{1}{\sqrt{\alpha_t}} \left( x_t - \frac{1-\alpha_t}{\sqrt{1-\alpha_t}} \epsilon_\theta(x_t, t) \right) + \sigma_t z$ 
end for
return  $x_0$ 

```

A.1.2 Annealed Langevin Dynamics Sampling

Algorithm 2 Annealed Langevin Dynamics Sampling [69]

```

Initialize  $x_0$ 
for  $i = 1, \dots, L$  do
   $\alpha_i \leftarrow \epsilon \cdot \sigma_i^2 / \sigma_L^2$ 
  for  $t = 1, \dots, L$  do
     $z_t \sim \mathcal{N}(0, I)$ 
     $\tilde{x}_t = \tilde{x}_{t-1} + \frac{\alpha_t}{2} s_\theta(\tilde{x}_{t-1}, \sigma_t) + \sqrt{\alpha_t} z_t$ 
  end for
   $\tilde{x}_0 \leftarrow \tilde{x}_T$ 
end for
return  $\tilde{x}_T$ 

```

A.1.3 Predictor-Corrector Sampling

Algorithm 3 Predictor-Corrector Sampling [66]

```

 $x_N \sim \mathcal{N}(0, \sigma_{\max}^2 I)$ 
for  $i = N - 1$  to  $0$  do
   $z \sim \mathcal{N}(0, I)$ 
  if Variance Exploding SDE then
     $x'_i \leftarrow x_{i+1} + \left( \sigma_{i+1}^2 - \sigma_i^2 \right) s_\theta * (x_{i+1}, \sigma_{i+1})$ 
     $x_i \leftarrow x'_i + \sqrt{\sigma_{i+1}^2 - \sigma_i^2} z$ 
  else if Variance Preserving SDE then
     $x'_i \leftarrow \left( 2 - \sqrt{1 - \beta_{i+1}} \right) x_{i+1} + \beta_{i+1} s_\theta * (x_{i+1}, i + 1)$ 
     $x_i \leftarrow x'_i + \sqrt{\beta_{i+1}} z$ 
  end if
  for  $j = 1$  to  $M$  do
     $z \sim \mathcal{N}(0, I)$ 
     $x_i \leftarrow x_i + \epsilon_i s_\theta * (x_i, \sigma_i) + \sqrt{2\epsilon_i} z$ 
  end for
end for
return  $x_0$ 

```

A.2 Conditional Sampling

A.2.1 Labeled Condition

Algorithm 4 Classifier-guided Diffusion Sampling [84]

```

Input: class label  $y$ , gradient scale  $s$ 
 $x_T \sim \mathcal{N}(0, I)$ 
for  $t = T, \dots, 1$  do
  if DDPM Sampling then
     $\mu, \Sigma \leftarrow \mu_\theta(x_t), \Sigma_\theta(x_t)$ 
     $x_{t-g} \leftarrow \text{sample from } \mathcal{N}(\mu + s\Sigma\nabla_{x_t} \log p_\phi(y | x_t), \Sigma)$ 
  end if
  if DDIM Sampling then
     $\hat{\epsilon} \leftarrow \epsilon_\theta(x_t) - \sqrt{1 - \bar{\alpha}_t} \nabla_{x_t} \log p_\phi(y | x_t)$ 
     $x_{t-1} \leftarrow \sqrt{\bar{\alpha}_{t-1}} \left( \frac{x_t - \sqrt{1 - \bar{\alpha}_t} \hat{\epsilon}}{\sqrt{\bar{\alpha}_t}} \right) + \sqrt{1 - \bar{\alpha}_{t-1}} \hat{\epsilon}$ 
  end if
end for
return  $x_0$ 

```

Algorithm 5 Classifier-free Guidance Sampling [280]

```

Input: guidance  $w$ , conditioning  $c$ , SNR  $\lambda_1, \dots, \lambda_T$ 
 $z \sim \mathcal{N}(0, I)$ 
for  $t = 1, \dots, T$  do
   $\tilde{\epsilon}_t = (1 + w)\epsilon_\theta(\mathbf{z}_t, \mathbf{c}) - w\epsilon_\theta(\mathbf{z}_t)$ 
   $\tilde{\mathbf{x}}_t = (\mathbf{z}_t - \sigma_{\lambda_t} \tilde{\epsilon}_t) / \alpha_{\lambda_t}$ 
   $\mathbf{z}_{t+1} \sim \mathcal{N}(\tilde{\mu}_{\lambda_{t+1}|\lambda_t}(\mathbf{z}_t, \tilde{\mathbf{x}}_t), (\tilde{\sigma}_{\lambda_{t+1}|\lambda_t})^{1-\nu} (\sigma_{\lambda_t|\lambda_{t+1}}^2)^\nu)$ 
end for
return  $\mathbf{z}_{T+1}$ 

```

A.3 Unlabeled Condition

Algorithm 6 Self-guided Conditional Sampling [93]

```

Input: guidance  $w$ , annotation map  $f_\psi, g_\phi$ , dataset  $\mathcal{D}$ , label  $\mathbf{k}$ , segmentation label  $\mathbf{k}_s$ , image guidance  $\hat{\mathbf{k}}$ 
 $x_T \sim \mathcal{N}(0, I)$ 
for  $t = T, \dots, 1$  do
   $z \sim \mathcal{N}(0, I)$ 
  if Self Guidance then
     $\tilde{\epsilon} \leftarrow (1 - w)\epsilon_\theta(x_t, t) + w\epsilon_\theta(x_t, t; f_\psi(g_\phi(\mathbf{x}; \mathcal{D}); \mathcal{D}))$ 
  else if Self-Labeled Guidance then
     $\tilde{\epsilon} \leftarrow \epsilon_\theta(x_t, \text{concat}[t, \mathbf{k}])$ 
  else if Self-Boxed Guidance then
     $\tilde{\epsilon} \leftarrow \epsilon_\theta(\text{concat}[x_t, \mathbf{k}_s], \text{concat}[t, \mathbf{k}])$ 
  else if Self-Segmented Guidance then
     $\tilde{\epsilon} \leftarrow \epsilon_\theta(\text{concat}[x_t, \mathbf{k}_s], \text{concat}[t, \hat{\mathbf{k}}])$ 
  end if
   $x_{t-1} = \frac{1}{\sqrt{\alpha_t}} \left( x_t - \frac{1-\alpha_t}{\sqrt{1-\alpha_t}} \tilde{\epsilon} \right) + \sigma_t z$ 
end for
return  $x_0$ 

```

**APPENDIX B
EVALUATION METRIC**

B.1 Inception Score (IS)

The inception score is built on valuing the diversity and resolution of generated images based on the ImageNet dataset [281], [282]. It can be divided into two parts: diversity measurement and quality measurement. Diversity measurement denoted by p_{IS} is calculated w.r.t. the class entropy of generated samples: the larger the entropy is, the more diverse the samples will be. Quality measurement denoted by q_{IS} is computed through the similarity between a sample and the related class images using entropy. It is because the samples will enjoy high resolution if they are closer to the specific class of images in the ImageNet dataset. Thus, to lower q_{IS} and higher p_{IS} , the KL divergence [283] is applied to inception score calculation:

$$\begin{aligned}
 IS &= D_{KL}(p_{IS} \parallel q_{IS}) \\
 &= \mathbb{E}_{x \sim p_{IS}} \left[\log \frac{p_{IS}}{q_{IS}} \right] \\
 &= \mathbb{E}_{x \sim p_{IS}} [\log(p_{IS}) - \log(q_{IS})]
 \end{aligned} \tag{49}$$

B.2 Frechet Inception Distance (FID)

Although there are reasonable evaluation techniques in the Inception Score, the establishment is based on a specific dataset with 1000 classes and a trained network that consists of randomness such as initial weights, and code framework. Thus, the bias between ImageNet and real-world images may cause an inaccurate outcome. Furthermore, the number of sample batches is much less than 1000 classes, leading to a value

FID is proposed to solve the bias from the specific reference datasets. The score shows the distance between real-world data distribution and the generated samples using the mean and the covariance [284].

$$FID = \|\mu_r - \mu_g\|^2 + \text{Tr} \left(\Sigma_r + \Sigma_g - 2(\Sigma_r \Sigma_g)^{1/2} \right) \tag{50}$$

where μ_g, Σ_g are the mean and covariance of generated samples, and μ_r, Σ_r are the mean and covariance of real-world data.

B.3 Negative Log Likelihood (NLL)

According to Razavi *et al.*, [285] negative log-likelihood is seen as a common evaluation metric that describes all modes of data distribution. Lots of works on normalizing flow field [286], [287] and VAE field [288], [289] uses NLL as one of the choices for evaluation. Some diffusion models like improved DDPM [61] regard the NLL as the training objective.

$$NLL = \mathbb{E} \left[-\log p_\theta(x) \right] \tag{51}$$

**APPENDIX C
BENCHMARKS**

The benchmarks of landmark models along with improved techniques corresponding to **FID score**, **Inception Score**, and **NLL** are provided on diverse datasets which includes CIFAR-10 [290], ImageNet [207], and CelebA-64 [291]. In addition, some dataset-based performances such as LSUN

[292], FFHQ [293], and MINST [294] are not presented since there is much less experiment data. The selected performance are listed according to NFE in descending order to compare for easier access.

C.1 Benchmarks on CelebA-64

TABLE 4
Benchmarks on CelebA-64

Method	NFE	FID	NLL
NPR-DDIM [108]	1000	3.15	-
SN-DDIM [108]	1000	2.90	-
NCSN [69]	1000	10.23	-
NCSN ++ [152]	1000	1.92	1.97
DDPM ++ [152]	1000	1.90	2.10
DiffuseVAE [116]	1000	4.76	-
Analytic DPM [107]	1000	-	2.66
ES-DDPM [101]	200	2.55	-
PNDM [76]	200	2.71	-
ES-DDPM [101]	100	3.01	-
PNDM [76]	100	2.81	-
Analytic DPM [107]	100	-	2.66
NPR-DDIM [108]	100	4.27	-
SN-DDIM [108]	100	3.04	-
ES-DDPM [101]	50	3.97	-
PNDM [76]	50	3.34	-
NPR-DDIM [108]	50	6.04	-
SN-DDIM [108]	50	3.83	-
DPM-Solver Discrete [64]	36	2.71	-
ES-DDPM [101]	20	4.90	-
PNDM [76]	20	5.51	-
DPM-Solver Discrete [64]	20	2.82	-
ES-DDPM [101]	10	6.44	-
PNDM [76]	10	7.71	-
Analytic DPM [107]	10	-	2.97
NPR-DDPM [108]	10	28.37	-
SN-DDPM [108]	10	20.60	-
NPR-DDIM [108]	10	14.98	-
SN-DDIM [108]	10	10.20	-
DPM-Solver Discrete [64]	10	6.92	-
ES-DDPM [101]	5	9.15	-
PNDM [76]	5	11.30	-

C.2 Benchmarks on ImageNet-64

TABLE 5
Benchmarks on ImageNet-64

Method	NFE	FID	IS	NLL
MCG [295]	1000	25.4	-	-
Analytic DPM [107]	1000	-	-	3.61
ES-DDPM [101]	900	2.07	55.29	-
Efficient Sampling [111]	256	3.87	-	-
Analytic DPM [107]	200	-	-	3.64
NPR-DDPM [108]	200	16.96	-	-
SN-DDPM [108]	200	16.61	-	-
ES-DDPM [101]	100	3.75	48.63	-
DPM-Solver Discrete [64]	57	17.47	-	-
ES-DDPM [101]	25	3.75	48.63	-
GGDM [115]	25	18.4	18.12	-
Analytic DPM [107]	25	-	-	3.83
NPR-DDPM [108]	25	28.27	-	-
SN-DDPM [108]	25	27.58	-	-
DPM-Solver Discrete [64]	20	18.53	-	-
ES-DDPM [101]	10	3.93	48.81	-
GGDM [115]	10	37.32	14.76	-
DPM-Solver Discrete [64]	10	24.4	-	-
ES-DDPM [101]	5	4.25	48.04	-
GGDM [115]	5	55.14	12.9	-

C.3 Benchmarks on CIFAR-10 Dataset

TABLE 6
Benchmarks on CIFAR-10 (NFE \geq 1000)

Method	NFE	FID	IS	NLL
Improved DDPM [61]	4000	2.90	-	-
VE SDE [66]	2000	2.20	9.89	-
VP SDE [66]	2000	2.41	9.68	3.13
sub-VP SDE [66]	2000	2.41	9.57	2.92
DDPM [68]	1000	3.17	9.46	3.72
NCSN [69]	1000	25.32	8.87	-
SSM [78]	1000	54.33	-	-
NCSNv2 [296]	1000	10.87	8.40	-
D3PM [65]	1000	7.34	8.56	3.44
Efficient Sampling [113]	1000	2.94	-	-
NCSN++ [152]	1000	2.33	10.11	3.04
DDPM++ [152]	1000	2.47	9.78	2.91
TDPM [99]	1000	3.07	9.24	-
VDM [67]	1000	4.00	-	-
DiffuseVAE [116]	1000	8.72	8.63	-
Analytic DPM [107]	1000	-	-	3.59
NPR-DDPM [108]	1000	4.27	-	-
SN-DDPM [108]	1000	4.07	-	-
Gotta Go Fast VP [109]	1000	2.49	-	-
Gotta Go Fast VE [109]	1000	3.14	-	-
INDM [121]	1000	2.28	-	3.09

TABLE 7
Benchmarks on CIFAR-10 (NFE < 1000)

Method	NFE	FID	IS	NLL
Diffusion Step [103]	600	3.72	-	-
ES-DDPM [101]	600	3.17	-	-
Diffusion Step [103]	400	14.38	-	-
Diffusion Step [103]	200	5.44	-	-
NPR-DDPM [108]	200	4.10	-	-
SN-DDPM [108]	200	3.72	-	-
Gotta Go Fast VP [109]	180	2.44	-	-
Gotta Go Fast VE [109]	180	3.40	-	-
LSGM [118]	138	2.10	-	-
DDIM [77]	100	4.16	-	-
FastDPM [105]	100	2.86	-	-
TDPM [99]	100	3.10	9.34	-
NPR-DDPM [108]	100	4.52	-	-
SN-DDPM [108]	100	3.83	-	-
DiffuseVAE [116]	100	11.71	8.27	-
DiffFlow [117]	100	14.14	-	3.04
Analytic DPM [107]	100	-	-	3.59
Efficient Sampling [113]	64	3.08	-	-
DPM-Solver [64]	51	2.59	-	-
DDIM [77]	50	4.67	-	-
FastDPM [105]	50	3.2	-	-
NPR-DDPM [108]	50	5.31	-	-
SN-DDPM [108]	50	4.17	-	-
Improved DDPM [61]	50	4.99	-	-
TDPM [99]	50	3.3	9.22	-
DEIS [113]	50	2.57	-	-
gDDIM [110]	50	2.28	-	-
DPM-Solver Discrete [64]	44	3.48	-	-
edm [112]	35	1.79	-	-
Efficient Sampling [113]	32	3.17	-	-
Improved DDPM [61]	25	7.53	-	-
GGDM [115]	25	4.25	9.19	-
NPR-DDPM [108]	25	7.99	-	-
SN-DDPM [108]	25	6.05	-	-
DDIM [77]	20	6.84	-	-
FastDPM [105]	20	5.05	-	-
DEIS [113]	20	2.86	-	-
DPM-Solver [64]	20	2.87	-	-
DPM-Solver Discrete [64]	20	3.72	-	-
Efficient Sampling [113]	16	3.41	-	-
NPR-DDPM [108]	10	19.94	-	-
SN-DDPM [108]	10	16.33	-	-
DDIM [77]	10	13.36	-	-
FastDPM [105]	10	9.90	-	-
GGDM [115]	10	8.23	8.90	-
Analytic DPM [107]	10	-	-	4.11
DEIS [113]	10	4.17	-	-
DPM-Solver [64]	10	6.96	-	-
DPM-Solver Discrete [64]	10	10.16	-	-
Progressive Distillation [62]	8	2.57	-	-
Denosing Diffusion GAN [63]	8	4.36	9.43	-
GGDM [115]	5	13.77	8.53	-
DEIS [113]	5	15.37	-	-
Progressive Distillation [62]	4	3.00	-	-
TDPM [99]	4	3.41	9.00	-
Denosing Diffusion GAN [63]	4	3.75	9.63	-
Progressive Distillation [62]	2	4.51	-	-
TDPM [99]	2	4.47	8.97	-
Denosing Diffusion GAN [63]	2	4.08	9.80	-
Denosing student [98]	1	9.36	8.36	-
Progressive Distillation [62]	1	9.12	-	-
TDPM [99]	1	8.91	8.65	-

TABLE 8
Details for Improved Diffusion Methods

Method	Year	Data	Model	Framework	Training	Sampling	Code
Landmark Works							
DPM [25]	2015	RGB Image	Discrete	Diffusion	L_{simple}	Ancestral	[code]
DDPM [68]	2020	RGB Image	Discrete	Diffusion	L_{simple}	Ancestral	[code]
NCSN [69]	2019	RGB Image	Discrete	Score	L_{DSM}	Langevin dynamics	[code]
NCSNv2 [296]	2020	RGB Image	Discrete	Score	L_{DSM}	Langevin dynamics	[code]
Score SDE [66]	2020	RGB Image	Continuous	SDE	L_{DSM}	PC-Sampling	[code]
Improved Works							
Progressive Distill [62]	2022	RGB Image	Discrete	Diffusion	L_{simple}	DDIM Sampling	[code]
Denosing Student [98]	2021	RGB Image	Discrete	Diffusion	$L_{Distill}$	DDIM Sampling	[code]
TDDP [99]	2022	RGB Image	Discrete	Diffusion	$L_{DDPM\&GAN}$	Ancestral	-
ES-DDPM [101]	2022	RGB Image	Discrete	Diffusion	$L_{DDPM\&VAE}$	Conditional Sampling	[code]
CCDF [95]	2021	RGB Image	Discrete	SDE	L_{simple}	Langevin dynamics	[code]
Franzese’s Model [103]	2022	RGB Image	Continuous	SDE	L_{DSM}	DDIM Sampling	-
FastDPM [105]	2021	RGB Image	Discrete	Diffusion	L_{simple}	DDIM Sampling	[code]
Improved DDPM [61]	2021	RGB Image	Discrete	Diffusion	L_{hybrid}	Ancestral	[code]
VDM [67]	2022	RGB Image	Both	Diffusion	L_{simple}	Ancestral	[code]
San-Roman’s Model [106]	2021	RGB Image	Discrete	Diffusion	$L_{DDPM\&Noise}$	Ancestral	-
Analytic-DPM [107]	2022	RGB Image	Discrete	Score	$L_{Trajectory}$	Ancestral	[code]
NPR-DDPM [108]	2022	RGB Image	Discrete	Diffusion	$L_{DDPM\&Noise}$	Ancestral	[code]
SN-DDPM [108]	2022	RGB Image	Discrete	Score	L_{square}	Ancestral	[code]
DDIM [77]	2021	RGB Image	Discrete	Diffusion	L_{simple}	DDIM Sampling	[code]
gDDIM [110]	2022	RGB Image	Continuous	SDE&ODE	L_{DSM}	PC-Sampling	[code]
INDM [121]	2022	RGB Image	Continuous	SDE	$L_{DDPM\&Flow}$	PC-Sampling	-
Ito-Taylor [23]	2021	RGB Image	Continuous	SDE	L_{DSM}	Ideal Derivatives Sampling	-
Gotta Go Fast [109]	2021	RGB Image	Continuous	SDE	L_{DSM}	Improved Euler	[code]
DPM-Solver [64]	2022	RGB Image	Continuous	ODE	L_{DSM}	Higher ODE solvers	[code]
edm [112]	2022	RGB Image	Continuous	ODE	L_{DSM}	2 nd Order Heun	[code]
PNDM [76]	2022	Manifold	Discrete	ODE	L_{simple}	Multi-step & Runge-Kutta	[code]
DDSS [115]	2021	RGB Image	Discrete	Diffusion	L_{simple}	Dynamic Programming	-
GGDM [111]	2022	RGB Image	Discrete	Diffusion	L_{KID}	Dynamic Programming	-
Diffusion GAN [63]	2022	RGB Image	Discrete	Diffusion	$L_{DDPM\&GAN}$	Ancestral	[code]
DiffuseVAE [116]	2022	RGB Image	Discrete	Diffusion	$L_{DDPM\&VAE}$	Ancestral	[code]
DiffFlow [117]	2021	RGB Image	Discrete	SDE	L_{DSM}	Langevin & Flow Sampling	[code]
LSGM [118]	2021	RGB Image	Continuous	ODE	$L_{DDPM\&VAE}$	ODE-Slover	[code]
Score-flow [119]	2021	Dequantization	Continuous	SDE	L_{DSM}	PC-Sampling	[code]
PDM [120]	2022	RGB Image	Continuous	SDE	L_{Gap}	PC-Sampling	-
ScoreEBM [122]	2021	RGB Image	Discrete	Score	$L_{Recovery}$	Langevin dynamics	[code]
Song’s Model [123]	2021	RGB Image	Discrete	Score	L_{DSM}	Langevin dynamics	-
Huang’s Model [129]	2021	RGB Image	Continuous	SDE	L_{DSM}	SDE-Solver	[code]
De Bortoli’s Model [128]	2021	RGB Image	Continuous	SDE	L_{DSM}	Importance Sampling	[code]
PVD [132]	2021	Point Cloud	Discrete	Diffusion	L_{simple}	Ancestral	[code]
Luo’s Model [33]	2021	Point Cloud	Discrete	Diffusion	L_{simple}	Ancestral	[code]
Lyu’s Model [34]	2022	Point Cloud	Discrete	Diffusion	L_{simple}	Farthest Point Sampling	[code]
D3PM [65]	2021	Categorical Data	Discrete	Diffusion	L_{hybrid}	Ancestral	[code]
Argmax [134]	2021	Categorical Data	Discrete	Diffusion	$L_{DDPM\&Flow}$	Gumbel sampling	[code]
ARDM [135]	2022	Categorical Data	Discrete	Diffusion	L_{simple}	Ancestral	[code]
Campbell’s Model [136]	2022	Categorical Data	Continuous	Diffusion	L_{simple}^{CT}	PC-Sampling	[code]
VQ-diffusion [137]	2022	Vector-Quantized	Discrete	Diffusion	L_{simple}	Ancestral	[code]
Improved VQ-Diff [138]	2022	Vector-Quantized	Discrete	Diffusion	L_{simple}	Purity Prior Sampling	[code]
Cohen’s Model [139]	2022	Vector-Quantized	Discrete	Diffusion	L_{simple}	Ancestral & VAE Sampling	[code]
Xie’s Model [140]	2022	Vector-Quantized	Discrete	Diffusion	$L_{DDPM\&Class}$	Ancestral & VAE Sampling	-
RGS [144]	2022	Manifold	Continuous	SDE	L_{DSM}	Geodesic Random Walk	-
RDM [145]	2022	Manifold	Continuous	SDE	L_{simple}^{CT}	Importance Sampling	-
EDP-GNN [148]	2020	Graph	Discrete	Score	L_{DSM}	Langevin dynamics	[code]
NCSN++ [152]	2021	RGB Image	Continuous	SDE	L_{DSM}	PC-Sampling	[code]

TABLE 9
Details for Diffusion Applications

Method	Year	Data	Framework	Downstream Task	Code
Computer Vision					
CMDE [27]	2021	RGB-Image	SDE	Inpainting, Super-Resolution, Edge to image translation	[code]
DDRM [201]	2022	RGB-Image	Diffusion	Super-Resolution, Deblurring, Inpainting, Colorization	[code]
Palette [97]	2022	RGB-Image	Diffusion	Colorization, Inpainting, Uncropping, JPEG Restoration	[code]
DiffC [202]	2022	RGB-Image	SDE	Compression	-
SRDiff [29]	2021	RGB-Image	Diffusion	Super-Resolution -	-
RePaint [203]	2022	RGB-Image	Diffusion	Inpainting, Super-resolution, Edge to Image Translation	[code]
FSDM [30]	2022	RGB-Image	Diffusion	Few-shot Generation	-
CARD [31]	2022	RGB-Image	Diffusion	Conditional Generation	[code]
GLIDE [85]	2022	RGB-Image	Diffusion	Conditional Generation	[code]
LSGM [118]	2022	RGB-Image	SDE	UnConditional & Conditional Generation	[code]
SegDiff [206]	2022	RGB-Image	Diffusion	Segmentation	-
VQ-Diffusion [137]	2022	VQ Data	Diffusion	Text-to-Image Synthesis	[code]
DreamFusion [205]	2023	VQ Data	Diffusion	Text-to-Image Synthesis	[code]
Text-to-Sign VQ [140]	2022	VQ Data	Diffusion	Conditional Pose Generation	-
Improved VQ-Diff [138]	2022	VQ Data	Diffusion	Text-to-Image Synthesis	-
Luo’s Model [33]	2021	Point Cloud	Diffusion	Point Cloud Generation	[code]
PVD [210]	2022	Point Cloud	Diffusion	Point Cloud Generation, Point-Voxel representation	[code]
PDR [34]	2022	Point Cloud	Diffusion	Point Cloud Completion	[code]
Cheng’s Model [133]	2022	Point Cloud	Diffusion	Point Cloud Generation	[code]
Luo’s Model [35]	2022	Point Cloud	Score	Point Cloud Denoising	[code]
VDM [26]	2022	Video	Diffusion	Text-Conditioned Video Generation	[code]
RVD [211]	2022	Video	Diffusion	Video Forecasting, Video compression	[code]
FDM [212]	2022	Video	Diffusion	Video Forecasting, Long-range Video modeling	-
MCVD [36]	2022	Video	Diffusion	Video Prediction, Video Generation, Video Interpolation	[code]
RaMViD [37]	2022	Video	SDE	Conditional Generation	-
Score-MRI [38]	2022	MRI	SDE	MRI Reconstruction	[code]
Song’s Model [213]	2022	MRI, CT	SDE	MRI Reconstruction, CT Reconstruction	[code]
R2D2+ [214]	2022	MRI	SDE	MRI Denoising	-
Sequence Modeling					
Diffusion-LM [39]	2022	Text	Diffusion	Conditional Text Generation	[code]
Bit Diffusion [40]	2022	Text	Diffusion	Image-Conditional Text Generation	[code]
D3PM [65]	2021	Text	Diffusion	Text Generation	-
Argmax [134]	2021	Text	Diffusion	Test Segmentation, Text Generation	[code]
CSDI [41]	2021	Time Series	Diffusion	Series Imputation	[code]
SSSD [42]	2022	Time Series	Diffusion	Series Imputation	[code]
CSDE [254]	2022	Time Series	SDE	Series Imputation, Series Predicton	-
Audio & Speech					
WaveGrad [43]	2020	Audio	Diffusion	Conditional Wave Generation	[code]
DiffWave [44]	2021	Audio	Diffusion	Conditional & Unconditional Wave Generation	[code]
GradTTS [45]	2021	Audio	SDE	Wave Generation	[code]
Diff-TTS [265]	2021	Audio	Diffusion	non-AR mel-Spectrogram Generation, Speech Synthesis	-
DiffVC [264]	2022	Audio	SDE	Voice conversion	[code]
DiffSVC [263]	2022	Audio	Diffusion	Voice Conversion	[code]
DiffSinger [46]	2022	Audio	Diffusion	Singing Voice Synthesis	[code]
Diffsound [259]	2021	Audio	Diffusion	Text-to-sound Generation tasks	[code]
EdiTTS [47]	2022	Audio	SDE	fine-grained pitch, content editing	[code]
Guided-TTS [48]	2022	Audio	SDE	Conditional Speech Generation	-
Guided-TTS2 [49]	2022	Audio	SDE	Conditional Speech Generation	-
Levkovitch’s Model [266]	2022	Audio	SDE	Spectrograms-Voice Generation	[code]
SpecGrad [50]	2022	Audio	Diffusion	Spectrograms-Voice Generation	[code]
ItoTTS [24]	2022	Audio	SDE	Spectrograms-Voice Generation	-
ProDiff [32]	2022	Audio	Diffusion	Text-to-Speech Synthesis	[code]
BinauralGrad [260]	2022	Audio	Diffusion	Binaural Audio Synthesis	-
AI For Science					
ConfGF [268]	2021	Molecular	Score	Conformation Generation	[code]
DGSM [53]	2022	Molecular	Score	Conformation Generation, Sidechain Generation	-
GeoDiff [54]	2022	Molecular	Diffusion	Conformation Generation	[code]
EDM [21]	2022	Molecular	SDE	Conformation Generation	[code]
Torsional Diff [55]	2022	Molecular	Diffusion	Molecular Generation	[code]
DiffDock [271]	2022	Molecular&protein	Diffusion	Conformation Generation, molecular docking	[code]
CDVAE [269]	2022	Protein	Score	Periodic Material Generation	[code]
Luo’s Model [56]	2022	Protein	Diffusion	CDR Generation	-
Anand’s Model [57]	2022	Protein	Diffusion	Protein Sequence and Structure Generation	-
ProteinSGM [270]	2022	Protein	SDE	de novo protein design	-
DiffFolding [275]	2022	Protein	Diffusion	Protein Inverse Folding	[code]